LBL-25529 c.2
Preprint

Lawrence Berkeley Laboratory
UNIVERSITY OF CALIFORNIA

Materials & Chemical Sciences Division

RECEIVED
LAWRENCE
BERKELEY LABORATORY
SEP 1988
LIBRARY AND
DOCUMENTS SECTION

Submitted to Chemical Physics

The Reactions of Ground and Excited State Sodium Atoms with Hydrogen Halide Molecules

P.S. Weiss, J.M. Mestdagh, M.H. Covinsky,
B.A. Balko, and Y.T. Lee

June 1988

TWO-WEEK LOAN COPY
This is a Library Circulating Copy
which may be borrowed for two weeks.

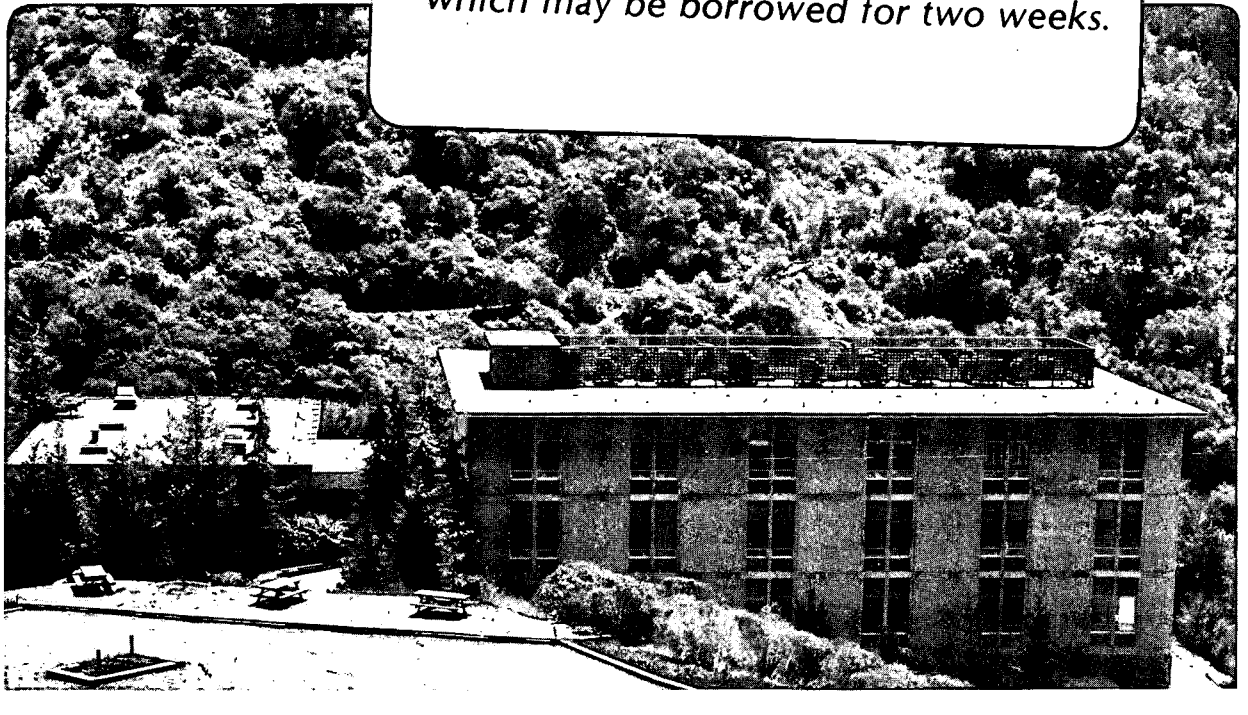

LBL-25529 c.2

Prepared for the U.S. Department of Energy under Contract Number DE-AC03-76SF00098.

DISCLAIMER

This document was prepared as an account of work sponsored by the United States Government. While this document is believed to contain correct information, neither the United States Government nor any agency thereof, nor the Regents of the University of California, nor any of their employees, makes any warranty, express or implied, or assumes any legal responsibility for the accuracy, completeness, or usefulness of any information, apparatus, product, or process disclosed, or represents that its use would not infringe privately owned rights. Reference herein to any specific commercial product, process, or service by its trade name, trademark, manufacturer, or otherwise, does not necessarily constitute or imply its endorsement, recommendation, or favoring by the United States Government or any agency thereof, or the Regents of the University of California. The views and opinions of authors expressed herein do not necessarily state or reflect those of the United States Government or any agency thereof or the Regents of the University of California.

THE REACTIONS OF GROUND AND EXCITED STATE SODIUM ATOMS WITH HYDROGEN HALIDE MOLECULES

P. S. Weiss,* J. M. Mestdagh,† M. H. Covinsky,
B. A. Balko, and Y. T. Lee

Materials and Molecular Research Division
Lawrence Berkeley Laboratory
and Department of Chemistry
University of California, Berkeley
Berkeley, CA 94720

ABSTRACT

The reactions of ground and excited state Na atoms with hydrogen halide (HX) molecules have been studied using the crossed molecular beams method. With both increasing translational and increasing electronic energy, the reactive cross sections increase in the reactions of HCl and HBr. From product angular and velocity distributions detailed center-of-mass information is derived. For the reactions of Na($3^2S_{1/2}$, $3^2P_{3/2}$, $4^2D_{5/2}$, $5^2S_{1/2}$) with HCl, the product NaCl is back-scattered with respect to the incoming Na atom in the center-of-mass frame of reference. The reaction of each Na state studied with HCl is direct and proceeds via collinear and near collinear Na-Cl-H approach geometries. For the Na($3^2P_{3/2}$) and Na($4^2D_{5/2}$) reactions with HCl the predominant transition state symmetry is $^2\Sigma$ in a collinear ($C_{\infty v}$) Na-Cl-H geometry. This is consistent with the reaction proceeding via electron transfer from the Na atom to the halide atom. Absolute reactive cross sections for each state of Na studied with HCl were determined by comparison with both small and large angle elastic scattering. We were unable to observe Na atoms with over 4 eV of electronic energy react with HF up to collision energies of 13 kcal/mole.

---

*Present address: IBM Research Division, Almaden Research Center, 650 Harry Road, San Jose, CA 95120

†Permanent Address: CEN Saclay, SPAS Bt. 62, 91191 Gif sur Yvette, CEDEX, France

I. Introduction

The reactions of alkali atoms (M) with hydrogen halide molecules (HX) have been studied in great detail.[1-28] Experiments have been performed in order to determine the dynamics of these reactions as well as the effects of reagent translational,[2-6] vibrational,[5-9] and rotational[8-10] excitation on the reaction. Until recently, the effect of electronic excitation remained unexplored.[11-14] With the appropriate choice of alkali and halogen atoms, the reaction can be made exothermic, thermoneutral, or endothermic.

Most of the theoretical studies of the reactions of alkali atoms with hydrogen halides have concentrated on Li+HF because of its relative simplicity. Chen and Schaefer have calculated an *ab initio* potential energy surface which shows an entrance channel well and an exit channel barrier which is lowest for a bent transition state.[15] Zeiri and Shapiro have extended their calculations of Li+HF to provide potential energy surfaces for 14 of the reactions in the alkali + hydrogen halide family.[16,17] They found that the barrier was lowest for a bent configuration in the M+HF potential energy surfaces, but was lowest for collinear and near collinear geometries in the M+HCl, HBr, HI potential energy surfaces.

NoorBatcha and Sathyamurthy performed quasiclassical trajectory calculations[19-21] on an analytic function fit to the Chen-Schaefer surface by Carter and Murrell.[22] They predicted a large (~1 eV) vibrational threshold to reaction, which was not found in the earlier crossed molecular beam experiments (in which essentially all of the HF and HCl molecules were in v=0).[2] They also predicted an initially decreasing then increasing dependence of reaction probability on rotational energy. This effect, although of a lower magnitude was seen in the experiments of Blackwell *et al.*[10]

Sevin *et al.* have calculated potential energy surfaces for Na(3S,3P,4S,4P,5S)+HF.[23] They found that for all the excited state processes exciplexes exist with stabilities of 0.5 eV for Na(3P) to over 1 eV for more highly excited Na states with respect to reactants. The exciplexes occur somewhat before the transition state on the ground state on the reaction

coordinate, which is rather steeply inclined at that point. Whether there is a possibility of proceeding to product NaF + H by this path is unclear from the calculations.

Gallo and Yarkony have calculated potential energy surfaces and their nonadiabatic coupling for $Na(3^2P,3^2P) + HCl$ in the same manner that Yarkony previously calculated for the reaction of $Li(2^2S,2^2P) + HCl$.[24,25] For $Na(3^2P) + HCl$ they found that there is a potential well in the entrance channel which is stable with respect to reactants by 0.24 eV and was nearly perpendicular (Na-Cl-H). Also, they found an exit channel barrier in the ground state surface that is bent at 55°. At approximately the same separation as the barrier, but with a larger Na-Cl-H angle, 100°, there was a maximum in the nonadiabatic coupling. This is important since excited state reactants do not correlate adiabatically to (energetically accessible) product NaCl + H, and thus switching onto the ground state surface is required for reaction.

A crossed molecular beams study was performed in our laboratory for the reactions $Li + HX \rightarrow LiX + H$ (X = F,Cl) in order to provide a test for theoretical calculations.[2] The Li + HF reaction proceeds with a low cross section, $\sigma_R < 1$ Å^2, yielding an average opacity of 0.1, at collision energies of 3 kcal/mole via a collision complex, and at 9 kcal/mole the lifetime of the collision complex appears to be shorter than the rotational period of the complex. Li + HCl had higher reactive cross sections, $\sigma_R > 25$ Å^2 and proceeds directly at the same collision energies, yielding an average opacity of 1.

Brooks and co-workers looked at the effect of translational energy on the K + HCl reaction.[4,5] They found an increase in reaction probability as the collision energy was increased from 3 to 10 kcal/mole, and then a fall-off as the collision energy was further increased to 18 kcal/mole. Heismann and Loesch, however, saw the reaction probability for $K + HX\ (v = 0,1) \rightarrow KX + H$ (X = F,Cl)[6] rise steadily until reaching a constant value for collision energies from approximately 20 kcal/mole up to over 40 kcal/mole. Lacmann and Herschbach studied K + HCl at collision energies of 1-20 eV, the production of K^+ was ob-

served only above the threshold for the appearance of both K^+ and Cl^-, but did not see $K^*(4P)$.[3] Balint-Kurti and Yardley have suggested that this was due to KCl molecules formed in very high vibrational levels which then dissociate to ion pairs.[26]

Odiorne, Brooks, and Kasper studied the effect of reagent vibrational excitation on the reaction $K + HCl\ (v=0,1) \rightarrow KCl + H$.[7] They found a rise in the estimated reaction cross section from $\sigma_R\ (v=0) = 0.15\ Å^2$ to $\sigma_R(v=1) = 20\ Å^2$, for a collision energy of 3-4 kcal/mole. Heismann and Loesch found similar results for $K + HCl\ (v=0,1)$ at low collision energies but saw a decrease in the vibrational enhancement with increasing collision energy.[6] The dropping off of the vibrational enhancement was due more to the increase in $\sigma_R(v=0)$ with increasing collision energy, than to a large drop in $\sigma_R(v=1)$, although there was a gentle decrease in $\sigma_R\ (v=1)$ at higher collision energies in the cases of both HCl and HF.

For rotational excitation in $K + HX(v=1,J) \rightarrow KX + H$, the reactive cross section decreased by a factor of 2 as J was increased from 1 to 4 for X=Cl.[9] By contrast, the cross section increased with J increasing from 5 to 7 for X=F.[8] This is as expected, from very low to moderate rotational excitation, the favored orientation for reaction is destroyed. With increasing rotational energy, the orientation is blurred due to fast rotation. Alternatively, this increase could be attributed to favorable excitation of bending in the transition state when the rotational angular momentum and the orbital angular momentum compensate which could help overcome the exit barrier to reaction. Blackwell, Polanyi, and Sloan looked at the reactions $Na + HX \rightarrow NaX + H$ for HX=HF (v=1-4, J=0-14), and HX=HCl (v=1-4, J=0-19) in a fascinating series of experiments that monitored the depletion of the infrared chemiluminescence of chemically produced HF and HCl by reaction with Na atoms. In comparing the reactivities of the various rotational levels within each vibrational level, they saw an initial decrease in reactivity with increasing J, and then a subsequent increase. The rotational energies achieved in this study were quite high. For HF, the maximum rotational energy was approximately 0.5 eV, or about one-fourth the energy of the first alkali electronic excitation, or about the energy of one HX vibrational quantum. It should be noted that for

Na + HF, a system discussed below, no depletion, and thus no reaction, was observed for HF(v = 1) which with a collision energy of >1.7 kcal/mole is energetically allowed to react to NaF + H.

The first crossed molecular beams study on the reaction of electronically excited sodium atoms was studied in our laboratory.[11] This was:

$$Na(nL) + HCl \rightarrow NaCl + H \qquad \Delta H_o^o = {}^{+}4.7 \text{kcal/mole}, \tag{1}$$

for which the reactive scattering of the ground ($3^2S_{1/2}$) and first excited ($3^2P_{3/2}$) states were studied. At a collision energy of 5.4 kcal/mole the ground state barely reacted due to the endothermicity of the process. The product NaCl had a broad angular distribution which was slightly back-scattered in the center-of-mass frame relative to the incoming Na atoms. This implies a direct reaction with collinear or near-collinear Na-Cl-H approach geometries required for reaction. Note that this is in contrast to the stable Na(3P)-ClH bent complex and transition state calculated in ref. [24] for this system. The product translational energy distribution was found to be broad and flat, remaining approximately constant from nearly zero translational energy up to all of the available energy going into translation. At high collision energy, 19.4 kcal/mole, where the reaction cross section becomes substantially larger, there was still an increase in reaction with electronic excitation, but the enhancement was clearly lower. This effect is similar to vibrational excitation, where enhancement is largest when the kinetic energy is near the threshold region.

Düren and coworkers have recently observed the reaction of Na(3^2P) + HF using a very sensitive hot wire detector.[14] They deconvoluted the inelastic Na atom scattering from the reactively scattered NaF by examining the time-of-flight spectra of the scattered particles. Although due to the kinematics of the system they were limited in the amount of forward-scattered product they could measure, they appear to have found symmetric forward-backward scattering consistent with the formation of a collision complex at a collision energy of 7 kcal/mole. They also measured the atomic orbital alignment dependence of the reaction

by rotating the polarization of the laser optically pumping the Na atoms, but saw only "very weak variations."[14]

The intention in performing the experiments of electronically excited sodium atoms with hydrogen halides described here was to enable a comparison between the effects of electronic excitation of sodium atoms on these reactions with the effects of other forms of energy already investigated. Specifically, how do the cross sections vary with electronic energy and the alignment of the electronically excited orbitals, and how are the reaction dynamics affected by varying electronic energy and the symmetry of the excited state?

II. Experimental

The basic crossed molecular beams apparatus has been described previously,[2,11-13,29,30] but several modifications were made to allow laser excitation at the crossing of the atomic and molecular beams.

Three types of experiments were performed: (1) product angular distributions were measured by rotating the detector about the collision region, (2) product velocities for fixed detector angles were measured using the time-of-flight method by modulating the product directly or the reaction itself by modulating the laser, and (3) the effect of rotating the laser polarization and thus the excited orbital alignment upon the reactive product at a fixed detector angle was measured.

Sodium vapor and a rare gas were mixed in an oven as described in refs. [12,13]. The Na-rare gas mixture was expanded through a stainless steel nozzle into a vacuum chamber maintained at $\sim 10^{-4}$ torr, through a stainless steel skimmer, into a differential pumping region, and finally into the collision chamber. The secondary molecular beam source was a heated stainless steel tube with a 70μ platinum nozzle on the end. The collision region was surrounded with a liquid nitrogen cold shield, and was typically at $\sim 10^{-7}$ torr. The volume of intersection of the beams was 1 x 3 x 3 mm^3. A triple differentially pumped ultrahigh

vacuum quadrupole mass spectrometer equipped with an electron bombardment ionizer and a Daly ion detector rotates about the collision region in the horizontal plane which includes the atomic and molecular beams.

Two optical windows mounted on the machine wall faced the secondary molecular beam source - one directly in the path of the molecular beam, and one 10″ below that. One or two dye laser beams entered through the lower window and were reflected up into the crossing region perpendicular to the scattering plane. The upper window was used for the collection of atomic fluorescence, as was a conflat viewport in the beam plane and in line with the detector when the detector was placed at 12.5° from the sodium atom beam in the direction of the secondary beam source.

Two other optical ports were each at 45° angles to the atomic and molecular beam axes at their crossing point in the beam plane so as to give a clear line of sight that passed through the crossing region. Each port had a Brewster window and a set of three sharp blackened apertures to spatially filter stray light. The laser was passed through these two ports in order to measure the Doppler profile of the Na D_2 line and thus the velocity profile of the sodium beam.

The optical pumping setup is shown in fig. 1. The Na($3^2P_{3/2} \leftarrow 3^2S_{1/2}$) D_2 transition was pumped by a cw single-frequency actively stabilized linear dye laser (Coherent Radiation Model 599-21) using Rhodamine 6G, pumped by 2.7 W at 5145 Å using an argon ion laser. This laser output 70-100 mW at the 5892 Å (yellow-orange) Na D_2 transition wavelength. A second transition from $3^2P_{3/2}$ was pumped by a cw single-frequency actively stabilized ring dye laser (Coherent Radiation Model 699-21/29) using Rhodamine 6G pumped with 6.0 W at 5145 Å with an argon ion laser. This was either the Na($5^2S_{1/2} \leftarrow 3^2P_{3/2}$) transition at 6162 Å (red, with 200-500 mW), or the Na($4^2D_{5/2} \leftarrow 3^2P_{3/2}$) transition at 5690 Å (green, with 400-800 mW). In some cases the laser frequencies were dithered $\pm$2-5 MHz at 510 Hz and 23 Hz, respectively, and locked to the peak of the fluorescence of the upper transition using lock-in amplifiers.

As shown in fig. 1 the two lasers were combined by having one laser beam nearly graze a mirror (M′) off the edge of which the other beam was reflected. The two beams were thus very nearly parallel and their overlap was maximized in the collision region (after a path length of greater than 3 m.) by maximizing the laser produced reactive signal. The two laser polarizations were kept parallel at all times. Each laser was monitored with a spectrum analyzer (FP) with a 1.5 GHz free spectral range. An iodine cell was used to determine the frequency of the laser using the iodine atlas of Gerstenkorn and Luc.[31] Approximately once an hour, a computer controlled shutter (S) sent a fraction of the 5890 Å light to the 45° Doppler crossing path in order to measure sodium beam velocity distributions. The lasers could be circularly polarized before being combined using a quarter-wave plate ($\lambda/4$) for the 5890 Å laser, and a Soleil-Babinet Compensator for the other laser. After being combined and before entering the main chamber the two lasers could be passed through a cross-correlation time-of-flight wheel.[32] Also, one or both of the lasers could be modulated at 3 Hz using a beam flag (not shown) run synchronously with the 150 Hz tuning fork secondary beam chopper which was located in the differential pumping region of the secondary beam source. The linear laser polarizations could be rotated in tandem using a computer controlled stepping motor driven double fresnel rhomb polarization rotator. As described above, the lasers entered the vacuum chamber parallel to and below the secondary beam, and were reflected up into the collision region from a mirror on the bottom of the machine. The fluorescence monitor positions were in line with the detector positions -12.5° and 90° (relative to the sodium beam).

The experiment was controlled by an LSI-11/23 computer. Angular and time-of-flight distributions and polarization dependences were recorded, and machine conditions were optimized using programs described in ref. [13].

Three sodium atomic beam energies were used. The rare gas backing pressures used were: 200-1000 torr for helium, 100-400 torr for neon, and 100-400 torr for argon. The large ranges were due predominantly to the various nozzle sizes at which measurements were made.

The atomic beam was seeded with gases of research grade purity (99.999%, Scientific Gases). The values of the peak velocity and speed ratio for the three backing gases commonly used are given in Table I. The secondary beam conditions used for the measurements are given in Table II.

Six channels of data were recorded simultaneously from two sources. The signal from the quadrupole mass spectrometer was recorded with the laser(s) and secondary beam on and off. Also, the signal from the fluorescence monitor was recorded with one (or both) laser(s) on and off. The reactions of four electronic states were measured. First, the Na(4D) versus Na(3P) distributions were measured with the yellow-orange (Na(3P←3S) transition) laser always on, and the green (Na(4D←3P) transition) laser modulated. Then, the Na(5S) versus Na(3S) distributions were measured by modulating the yellow-orange (Na(3P←3S) transition) and the red (Na(5S←3P) transition) lasers with the beam flag.

The signal due purely to the excited state (EXC) is:

$$\mathrm{EXC} = \frac{(L_{on}B_{on} - L_{on}B_{off}) - [(1 - \mathrm{FE})(L_{off}B_{on} - L_{off}B_{off})]}{\mathrm{FE}}, \tag{2}$$

where $L_{on/off}B_{on/off}$ are the mass spectrometer signals with the laser (L) and the secondary beam (B) on or off, and FE is the fraction excited. Note that the contribution due to the fraction remaining in the lower state with the laser on (1-FE) is removed. To counteract the effects of long term drifts in machine conditions, an angle - usually the peak of the reactive signal - was chosen for the normalization of the data. After every ten measurements at various angles, measurement at this reference angle was carried out. The time at which each measurement was taken was recorded, and the data was normalized by taking a linear interpolation in time between successive sets of normalization measurements.

Polarization measurements were recorded with the addition of a broadband polarization rotator (Spectra Physics 310A). This polarization rotator was mounted to a stepping motor (Slo-Syn M062-FC09E) driven by a CAMAC pulse generator (Kinetic Systems 3360). As

with angular distributions the measurements were made for 60 seconds in real time. Note that each polarization rotation measurement was made with the detector held at a fixed angle. By using the upper laser entry window, the laser polarization could also be rotated out of the scattering plane.

The favored polarization angle ϕ and the amplitude of the polarization dependence (2A) were determined by fitting a cosine curve of the form:

$$\text{Normalized Signal} = A\cos(2(\theta - \phi)) + (1 - A) \tag{3}$$

to the reactive signal. The same was done for the fluorescence signal for the signal from a fixed fluorescence monitor in the plane of the scattering. This fluorescence amplitude provides a direct measure of the fraction of atoms aligned as discussed in ref. [13]. The fit of equation (3) to the fluorescence data gave the amplitudes as $2A = 0.35$ for the 3P excitation, and $2A = 0.32$ for the 4D excitation.

The time-of-flight (TOF) measurements for product velocity distributions reported here were made by modulating the laser with a pseudo-random binary sequence of 255 photoetched slots on a wheel which spun at 392 Hz to give a time resolution of 10 μsec over the 20.8 cm flight path of the reaction products. The TOF spectra were recorded on a CAMAC 4096 channel scaler described in ref. [13]. As discussed in ref. [11], the laser modulation has the disadvantage of modulating any signal due to ground state in the opposite direction, and this data must be either measured or accurately synthesized in order to be taken into account in the subsequent data analysis.

The data was transformed from the laboratory frame of reference in which it was recorded to the center-of-mass (cm) frame of reference in which it is easily interpretable by the forward convolution method taking into account the experimental resolutions.[33,34] The

parameters for the cm distributions were varied iteratively in order to minimize the differences of the measured and calculated laboratory angular and velocity distributions.

The relevant Na atomic energy levels are shown in fig. 2. The fine and hyperfine structure are not shown in this figure. The three upward pointing arrows show the essential transitions optically pumped. The Einstein A coefficients for these transitions have been measured experimentally [35] and calculated [36] for all the states relevant to the present study. To pump the Na($3^2P_{3/2}$) state a single laser was tuned to the 16973.379 cm^{-1} (yellow-orange) Na($3^2P_{3/2}$, F = 3 ← $3^2S_{1/2}$, F = 2) transition. In order to pump the $5^2S_{1/2}$ state, a second laser was tuned to the 16227.317 cm^{-1} (red) Na($5^2S_{1/2}$, F = 2 ← $3^2P_{3/2}$, F = 3) transition. To pump the $4^2D_{5/2}$ state, the second laser was tuned to the 17575.410 cm^{-1} (green) Na($4^2D_{5/2}$, F = $3^2P_{3/2}$, F = 3) transition. Note that in pumping the $5^2S_{1/2}$ and $4^2D_{5/2}$ states, the 4S and 4P states were radiatively populated. The details of the laser excitation of sodium have been discussed by Hertel and co-workers.[37,38]

Experiments on reactive scattering have shown that having both lasers circularly polarized in the same sense yielded a Na(4D) fraction approximately 15% higher than having both lasers linearly polarized with their electric vectors parallel. If the two lasers were circularly polarized with the opposite sense, the fraction excited was reduced by more than a factor of 3. Several of the product angular distributions of the reactive scattering of Na(4D) atoms were performed with both the linear and circular polarization optical pumping schemes, and no fundamental differences were observed between the cases. No polarization dependence of the reactive scattering at a single detector angle of greater than 17% was seen, so this should limit the effect on the angular distributions recorded.

For the reactive scattering experiments of the 4D state, it was not possible to separate the contributions of the radiatively populated 4S and 4P states. Thus, the angular distrib-

utions derived for the 4D state in general contain the contributions of these states. No experiments were done to directly excite the Na(4S,4P) states. For the distributions, it was assumed that (1) the excited state fraction in the 3P state remained unchanged when the second laser was added, (2) the ground state contribution to the reactive scattering of the ground state was negligible, and (3) the fraction excited to the 4D state was 80% that to the 3P state. Assumption (1) is based on the experimental observation that the fluorescence from the 3P did not change when the second laser excitation was modulated. Assumption (2) is an empirical observation. Assumption (3) is based on the estimates of Jamieson *et al.*[39] The scattering due to the Na(4D) state was determined as:

$$4D = (ON4D - OFF3P) / 0.8, \tag{4}$$

where 4D is the signal due to the Na(4D) state, ON4D is the signal with both lasers on, OFF3P is the signal with the green laser off and the yellow laser on (so that the 3P level was still excited).

As in the 4D case, a second dye laser can be used to excite from the $3^2P_{3/2}$ level to the $5^2S_{1/2}$ level. The $5^2S_{1/2}$ level can fluoresce into both the fine structure states of the 3P and 4P states (the branching ratio is 0.5:1.0:0.4:0.7 for: $3^2P_{1/2}$:$3^2P_{3/2}$:$4^2P_{1/2}$:$4^2P_{3/2}$. There is no simple way to avoid fluorescence into dark levels, but as pointed out by Jamieson *et al.*,[39] and observed here, there does not seem to be a large difference in the pumping efficiency of this level relative to pumping the 4D level.[39] Linearly polarized lasers whose electric vectors were parallel were used to pump the transitions. Estimates by Jamieson *et al.* for the fraction in each state with excitation to the 5S state are shown as the bracketed quantities in fig. 2.

As with the 4D state, it was not possible to separate the contributions to the reactive scattering by the radiatively populated 4S and 4P states. Thus, the distributions derived for the 5S state also contain the contributions of these states. The same assumptions regarding

the excitation were made as for the excitation of the 4D state as in equation (4) *mutatis mutandis*.

III. Results

1. Na(4D,5S) + HCl

When excited to the Na($4^2D_{5/2}$, $5^2S_{1/2}$) states and reacted with HCl in crossed molecular beams, the NaCl product angular and velocity distributions change substantially from what was observed for the Na($3^2P_{3/2}$) + HCl reaction. Angular distributions for:

$$\mathrm{Na(3S, 3P, 4D, 5S) + HCl \rightarrow NaCl + H} \qquad \Delta H_0^\circ = {}^{+}4.7 \text{ kcal/mole.}^{[40]} \tag{5}$$

were measured at collision energies of 3.4, 5.6, and 16.3 kcal/mole. Newton velocity vector diagrams detailing the kinematics of the system at these three collision energies are shown in fig. 3. The angular distributions themselves are shown in figs. 4-6. The distributions shown are the raw data - the 4D and 5S curves include the contributions of 3S and 3P as well as the radiatively populated 4S and 4P states. Two dramatic effects are immediately apparent: the angular distributions have narrowed, and the signals at the peak have increased in going from Na(3P) to Na(4D,5S). TOF measurements for Na(4D,5S)+HCl at a collision energy of 5.6 kcal/mole are shown for various detector angles in figs. 7 and 8, respectively. The TOF distributions include the contribution of Na(3P) also, as well as the negative contribution due to the depletion of the ground state as discussed in ref. [11]. These measurements confirm that there is actually less translational energy in the NaCl due to the reaction of Na(4D,5S) than that due to Na(3P).

At a collision energy of 5.6 kcal/mole for Na(4D)+HCl, the dependence of the reactive signal at several detector angles upon the laser polarization was measured as described above. The derived distributions are shown in fig. 9 and summarized in Table III. As seen in Table

III, at all detector angles measured the favored polarization angles for reaction were within a few degrees of the relative velocity vector of the system.

Simultaneously recorded polarization dependences for Na(3P)+HCl showed no observable polarization dependence except for the farthest back-scattering (at a laboratory detector angle of 56° for which a 3% dependence (2A=0.03) was observed favoring reaction when the laser polarization was parallel to the relative velocity vector. In previous measurements, no effect was seen for Na(3P)+HCl, but the minimum detectable effect for those measurements was 10-15%, so that it is not surprising that nothing was seen.[11] The upper limit of any polarization dependences for the other angles (30°-50°) for which none were observed could safely be put at 2%.

2. Na + HF

At collision energies up to 13.4 kcal/mole no reaction was observed for:

$$\mathrm{Na(3S,3P,4D,5S)} + \mathrm{HF} \rightarrow \mathrm{NaF} + \mathrm{H} \qquad \Delta H_o^o = {}^{+}13.\ \mathrm{kcal/mole.}^{[40]} \tag{6}$$

Extensive signal averaging yielded no detectable NaF within the angular limits defined by its kinematics at m/e=42 (NaF^+) nor at m/e=23 (Na^+). As mentioned above, reaction of $Na(3^2P)$+HF was observed by Düren *et al.* with a very sensitive detector,[14] as well as for ground state sodium atoms with vibrationally excited HF ($v \geq 2$) in chemiluminescence experiments by Blackwell *et al.*[10]

3. Na(3S,3P) + HBr

Angular distributions have been measured for the reaction:

$$\mathrm{Na(3S,3P)} + \mathrm{HBr} \rightarrow \mathrm{NaBr} + \mathrm{H} \qquad \Delta H_o^o = {}^{+}0.4\ \mathrm{kcal/mole}^{[40]} \tag{7}$$

at collision energies of 3.0, 5.3, and 20.0 kcal/mole, as shown in figs. 10, 11, and 12, respectively. Being very nearly thermoneutral in the absence of electronic and collision energy, a substantial amount of ground state reaction was observed for each collision energy studied. Still, there was a significant increase in the reactive cross section for the reaction when the Na atoms were excited to the 3P state.

IV. Analysis of Experimental Results

Experimental angular and TOF distributions were fitted using the forward convolution method by varying independent cm scattering angular and translational energy distributions of products in the center-of-mass coordinate system. The best fits to the measured angular distributions for Na(4D)+HCl and Na(5S)+HCl obtained for the 5.6 kcal/mole collision energy are shown in fig. 13. The fits of the same cm distributions to the TOF data are shown in figs. 7 and 8 for Na(4D)+HCl and Na(5S)+HCl, respectively.

A comparison of the best fit translational energy distributions ($P(E'_T)$ distributions) at collision energies of 5.4 kcal/mole for Na(3P), and 5.6 kcal/mole for Na(4D) and Na(5S) in fig. 14 points up this large change in the dynamics of the reaction. Note that with increasing electronic energy, the peaks and the mean energies in the $P(E'_T)$ distributions move to lower energy, with $E'_{T,peak}$ = 16, 7, and 4 kcal/mole and $< E'_T >$ = 20, 7, and 7 kcal/mole for the reactions of the 3P, 5S, and 4D, respectively. The tails of the recoil energy distributions in all cases go out to the maximum possible energy available.

The calculated cm angular distributions ($T(\theta)$) are shown in fig. 15 for the product NaCl due to Na(5S) and Na(4D) at 5.6 kcal/mole. These are similar to the $T(\theta)$ found for the reaction of the Na(3P) atoms in ref. [11]. The NaCl due to the Na(4D,5S) states show backwards peaking with over 70% scattered into the backwards hemisphere versus just over

50% for NaCl due to Na(3P) reaction. The features of the two upper state $T(\theta)$ distributions are sharper and exhibit a sharp rise at approximately 90° for each.

The relative integrated cross sections for the reaction at 5.6 kcal/mole increase with increasing electronic energy. The ratios of integrated cross sections for the excited electronic states are:

6.2 (4D): 4.3(5S): 1.0 (3P) at 5.6 kcal/mole.

As in equation (4), a relative optical pumping efficiency of 0.8 for the upper state (4D or 5S) as compared to the 3P state was assumed, and the fraction of atoms in the Na(3P) state was assumed unchanged when the second laser was turned on.

Assuming 20% efficiency in optically pumping the Na(3P) state from the ground state, the following ratios of reactive cross sections were obtained:

115 (3P) : 1 (3S) at 5.4 kcal/mole, and

6 (3P) : 1 (3S) at 16.3 kcal/mole.

The 20% pumping efficiency is a liberal estimate, particularly in the most difficult to pump case of Na seeded in He (E_{coll} = 16.3 kcal/mole). If the pumping efficiency were lower, the enhancements would be larger than those reported above. Also, by lowering the collision energy below the endothermicity of the reaction, the enhancement could be made arbitrarily large; at 3.4 kcal/mole, this measured ratio was in fact infinite because of the lack of reaction of Na(3S).

The absolute reactive cross sections can be estimated by comparison with small angle elastic scattering.[42] This method eliminates the need to know the reactant beam number densities at the interaction region - difficult quantities to determine accurately. Also, since both elastically scattered Na and reactively scattered NaCl can be observed at m/e = 23 (as Na^+), only the relative probability of ionization of the two species to Na^+ needs to be known, rather than the exact ionization efficiencies and the transmission functions of the

quadrupole mass spectrometer at two different masses. The cross sections determined have an accuracy of no better than a factor of two. The estimated cross sections for the reaction at a collision energy of 5.6 kcal/mole are given in Table IV.

The absolute cross section can also be estimated by comparison with large angle elastic scattering which is attributable to low impact parameter collisions. A hard sphere collision is assumed which leads to isotropically scattered products if the impact parameter of the collision is smaller than the sum of the spheres' radii. The sum of the radii is equivalent to the classical turning point of the Na-HCl potential curve, which by analogy to $He^*(2^1S) + Ar$ is estimated to be 3 Å at a collision energy of 5 kcal/mole.[43] This gives a hard sphere cross section of 28 Å^2. The values of the absolute reactive cross section obtained in this way are shown in the right hand column of Table IV, and agree reasonably well with the values obtained from the small angle elastic scattering.

V. Discussion

1. The Mechanism and Product Energy Distribution in the Na(4D,5S)+HCl Reaction

The dominant features of the Na^* + HCl scattering are the decreasing product translational energy and the increasing reactive cross section with increasing electronic energy.

While an electron jump mechanism has never before adequately explained the dynamics of an alkali-hydrogen halide reaction,[11] the very low ionization potential of the highly excited alkali atoms could increase the effect of such a process. HCl^- is known to be dissociative.[44] HCl is dissociated by electrons with relatively low energies, and dissociative electron attachment measurements yield an estimated (negative) vertical electron affinity of -0.815 eV.[44] Thus if an electron transfers from the sodium atom to the HCl at long range, the HCl^- could quickly dissociate. Since the H atom is so much lighter than the Cl^- ion, the H atom will rapidly depart, if the effect of the Na^+ is ignored. The Na^+ and the Cl^- ions are then left at a separation approximately equal to the electron jump radius.

If an electron jump mechanism is assumed, then the largest impact parameter leading to reaction would be the same as the position of the crossing of the neutral and ionic potential energy curves. By neglecting the long range neutral attractions, this can be estimated by:

$$IP - EA = \frac{e^2}{r_c}, \tag{8}$$

where IP is the ionization potential of the appropriate sodium level, EA is the electron affinity of the HCl molecule and r_c is the crossing radius of the neutral and ionic curves.[45,46] For the four electronic states of sodium studied, this yielded the values of r_c shown in table V.

As pointed out in ref. [11], the electronic transfer radii for the Na(3S,3P) states are too small to be able to separate the breakage of the HCl bond (by electron transfer) from the formation of the NaCl bond. By the time the electron transfers from the alkali atom, the H atom already feels the repulsion of the closed shell NaCl molecule that is being formed. With the larger electron transfer radii of the Na(4D,5S) states, this is no longer the case. The H atom feels only the repulsion of the closed shell Cl^- atom.

If the orientation of the HCl is not important, the electron transfer cross section (σ_e) is expected to be:

$$\sigma_e = \pi r_c^2. \tag{9}$$

The values of σ_e are given in the right-hand column of table V.

The cm NaCl angular distributions derived for the reactions of Na(4D,5S) with HCl lead to the conclusion that the opacity function (the reaction probability as a function of impact parameter) was not $P(b) = 1$ for all $b < r_c$. That is, not all encounters close enough for electron transfer led to chemical reaction. The relatively strong back-scattering implies that the favorable configuration for reaction (of Na(4D,5S)) was Na-Cl-H.

The values of $\sigma_R(3P)$, $\sigma_R(4D)$, and $\sigma_R(5S)$ shown in table V are all significantly lower than the electron transfer cross sections given in table V. Also, note that the relative cross sections do not go up as the square of the crossing radii. This is indicative of what is already known from the cm angular distributions -- the importance of the orientation of HCl with respect to the approaching Na atom which causes the opacity function P(b) to be significantly less than 1 for $b < r_c$.

Evidence that electron transfer takes place at distances much larger than the impact parameter of most of the reactive collisions comes from the polarization dependences. All favored laboratory polarization angles ϕ_{LAB} were near the angle of the relative velocity vector as shown in fig. 9 and table III. This is made clear in the ϕ_{CM} values, which are the angles between the favored laboratory polarization angles and the angle of the relative velocity vector of the system in the laboratory frame of reference. This is in sharp contrast to the lack of noticeable polarization dependences seen for Na(3P)+HCl. In the limiting case of $C_{\infty v}$ (collinear) geometry the required symmetry for reaction to form the ionic NaCl is $^2\Sigma$ since the ion pair derives this symmetry from:

$$Na^+(^1S) + HCl^-(^2\Sigma^+) \tag{10}$$

Because of the ground state $HCl^-(X^2\Sigma^+)$ symmetry, all electronic angular momentum of the Na(4D) must be perpendicular to the Na-Cl-H axis -- requiring the $4d_{z^2}$ orbital to be along the Na-Cl-H axis.

If this collinear geometry and $^2\Sigma$ symmetry were a strict requirement for reaction, then as the impact parameter was raised the Na-Cl-H orientation (axis) required for reaction would tilt with respect to the relative velocity vector. In the impulsive reaction limit, this would lead to lower cm (NaCl) scattering angles and thus lower laboratory scattering angles. Also, this would imply that the favored polarization for reaction would rotate with respect to the relative velocity vector to match the Na-Cl-H axis. Of course, since different impact parameters would lead to different reactive orientations and different scattering angles, the

polarization dependence would vary as a function of laboratory scattering angle. This was not observed. Therefore, the assumption of collinearity and/or the impulsive approximation that the scattering angle depends upon the impact parameter are incorrect if larger impact parameters lead to reaction. From the backwards-peaked NaCl angular distributions we deduce that only small impact parameters lead to reaction, and thus the reactive collisions are not impulsive.

Two features observed imply that the Na(4D,5S)+HCl reaction proceeded through long range electron transfer and early H atom departure, even though only in a limited set of orientations and impact parameters. These are the very low product recoil energy, and the polarization dependences for the reaction of Na(4D) versus the lack of a polarization dependence for the reaction of Na(3P). That the reaction occurred through early departure of the H atom, but only for small impact parameter collisions, indicates that a coupling of nuclear and electronic motions was required for reaction. Otherwise, any trajectory for which electron transfer was energetically possible (i.e. for $b < r_c$) would have led to reaction.

Three other processes were energetically possible under the conditions studied in the collisions of Na^* with HCl. It was possible to have the reaction proceed to form NaH:

$$Na + HCl \rightarrow NaH + Cl \qquad \Delta H_0^o = {}^+58.8 \text{ kcal/mole.}^{[40]} \tag{11}$$

It was also possible to collisionally dissociate HCl:

$$Na + HCl \rightarrow Na + Cl + H \qquad \Delta H_0^o = {}^+102.2 \text{ kcal/mole.}^{[40]} \tag{12}$$

The third set of energetically possible processes involves quenching to other electronic states of Na:

$$Na(nL) + HCl \rightarrow Na(nL) + HCl(v,J). \tag{13}$$

The electronic energies available for reaction were 98.8 kcal/mole and 94.9 kcal/mole for the 4D and 5S states of Na, respectively. Both these energies are more than sufficient for

the production of NaH (process (11)). However, no evidence for the production of NaH was observed. This is not surprising; if electron transfer occurs at relatively long range, the H atom is quickly ejected as a neutral, before encountering the alkali ion. Another interpretation has the electronically excited alkali atom acting as an alkali ion when close to the hydrogen halide. This is helpful in explaining the alkali favoring the halide end of the HX molecule on approach, as seen in the strong variation of the barrier to (ground state) reaction as a function of M-X-H angle calculated by Shapiro and Zeiri; the barrier rises several eV as the orientation approaches the M-H-X collinear configuration.[17] The long range dispersive forces alone would have the alkali atom favoring the hydrogen end of the molecule.[11,28]

With collision energies of at least 3.5 kcal/mole and 7.0 kcal/mole, respectively, the 4D and 5S states of Na have enough energy to dissociate HCl (process (12)). For a reactive system, a better way of looking at collisional dissociation is perhaps as reaction to form NaCl above its dissociation limit. Apparently, at the range of collision energies studied, sufficient energy was carried away by product translation and collision dissociation does not seem to have been important.

Quenching (process (13)) certainly occurs, but our measurements were particularly insensitive to it. Therefore, quenching processes have not been investigated in these studies. Hertel and coworkers, among others, have performed many experiments on the quenching of excited sodium atoms by various diatomic molecules (although no hydrogen halides have been reported to date), and the quenching cross sections are typically quite large $\sim O(10\text{-}100\ \text{Å}^2)$.[38]

2. Na(3S,3P) + HBr

The Na + HBr reaction is nearly thermoneutral and there is a substantial cross section for ground state reaction. However, the reactive cross section increased upon excitation of the Na atoms to the 3P level. As with Na + HCl, the ground state cross section increased

more with increasing collision energy than the cross section of the Na(3P) state. This data is very similar to the Na(3P)+HCl data, where product NaX was mostly back-scattered, but there was some forward and sideways scattered products, and the product recoil energy distributions were broad and flat, once again extending out to the total energy available.

3. The Lack of Reaction for Na+HF

We observed no reaction for Na(3S,3P,4D,5S)+HF. For comparison, recall that it took two vibrational quanta of HF excitation for Blackwell *et al.* to observe evidence of reaction to form NaF.[10] Düren *et al.* did observe formation of NaF from Na(3P)+HF with their hot wire detector.[14] It appears likely that the cross section was too small for us to observe NaF using electron bombardment ionization. There are no close resonances for electronic to vibrational energy transfer of HF that might reduce the reaction probability in the manner suggested by Zeiri *et al.* for translational to vibrational energy transfer in Li+HF.[18] The vertical electron affinity of HF is approximately -4 eV and like HCl^-, HF^- is dissociative.[41] The crossing point of the neutral and ionic curves, and thus electron transfer occurs at under 3 Å for the 4D and 5S states. Therefore, even for Na(4D,5S)+HF an increased reaction cross section due to long range electron transfer is not expected.

VI. Conclusions

The electronic excitation of the reagent alkali atom can indeed promote reaction. As seen in Na(4D,5S)+HCl, a new mechanism comes to dominate the reaction at high electronic energy, although the reactive cross sections did not reach the limit in which all collisions for which electron transfer was possible led to reaction. This is due to the restrictive geometric constraints necessary for reaction. Low impact parameter collisions with Na approaching the Cl end of the HCl molecule were almost exclusively responsible for production of NaCl, since a coupling of the electronic and nuclear motion was necessary for reaction.

Electronic excitation is not directly comparable to other forms of energy since the potential energy surface on which the reaction takes place is different for each electronic state -- with different topography and different possible symmetries. Nevertheless it is certainly interesting to ask how electronic excitation compares to other forms of energy in promoting reaction. Like electronic energy, exciting the first (or second) vibration is capable of turning on the reaction when the collision energy is insufficient to overcome the endothermicity. This was shown for K + HF,HCl[6] (and for Na + HF(v = 2)[10]). As discussed in section I and ref. [6], with increasing translational energy the first vibration in K + HCl no longer enhances the reaction cross section, whereas there is over an order of magnitude enhancement in K + HF. Rotational excitation has only been studied in vibrationally excited HCl,HF + Na,K, and seems to adversely affect the reaction cross section or have little effect.[8-10] Translational energy overcomes the threshold to reaction in K + HCl,HF and continues to enhance reaction until a saturated value of the cross section is reached.[6] In Na + HCl,HBr the initial electronic excitation to Na(3P) enhanced reactivity strongly whether or not there was sufficient collision energy for the ground state reaction. Düren *et al.* also showed that electronic energy could overcome the endothermicity of the Na + HF reaction.[14] In Na + HCl, there was a further increase with further increased electronic energy.

Acknowledgements

The authors gratefully acknowledge useful discussions with H. Schmidt. The authors would also like to thank Ms. Isabelle Duborg for help in the preparation of the figures, and Ms. Maura O'Neill for help in the preparation of the manuscript. This work was supported by the Director, Office of Energy Research, Office of Basic Energy Sciences, Chemical Sciences Division of the U.S. Department of Energy under Contract No. DE-AC03-76SF00098. Some of the lasers used in these experiments were on loan from the San Francisco Laser Center supported by the NSF under grant No. CHE79-16250 awarded to the University of California at Berkeley in collaboration with Stanford University.

Table I. Measured sodium beam velocities and speed ratios, and calculated maximum transverse sodium velocities and the resultant Doppler broadening of the Na D_2 transition.

Seed Gas	Sodium Peak	Maximum Transverse Velocity (in 10^4 cm/sec)	Speed Ratio	Doppler Broadened Linewidth (in MHz)
Helium	30.0	3.3	6	56
Neon	16.0	1.8	5	30
Argon	10.8	1.2	5	20

Table II. Velocities and speed ratios for molecular beams used in reactive scattering studies.

Reactant Beam	Nozzle Temperature (in °C)	Beam Velocity (in 10^4 cm/sec)	Speed Ratio
HBr	200	5.8 (est.)	4
HCl	179	8.6	4.5
HF	250	12.3 (est.)	4.6

Table III. A summary of the polarization dependences found for the reaction $Na(4^2D_{5/2}) + HCl \rightarrow NaCl + H$ at a collision energy of 5.6 kcal/mole. These results are tabulated from figure 9.

Laboratory Detector Angle	Laboratory Peak of Polarization Dependence ϕ_{LAB}	Center-of-Mass Peak of Polarization Dependence ϕ_{CM}	Amplitude
35°	163°	13°	0.112
40°	158°	8°	0.080
44°	155°	5°	0.112
50°	158°	8°	0.098
56°	147°	-3°	0.170

Table IV. Estimated total reaction cross sections (σ_R) for Na(3S,3P,4D,5S) + HCl at a collision energy of 5.6 kcal/mole from the elastic scattering of Na(3S,3P) atoms and estimates of the absolute cross sections from Van der Waals attraction at small angles, and hard sphere collisions at large angles.

Electronic State	σ_R from Na(3S) Scattering at Small Angles (in Å^2)	σ_R from Na(3P) Scattering at Small Angles (in Å^2)	σ_R from Na(3S) Scattering at Large Angles (in Å^2)
3S	0.034	0.017	0.057
3P	4.0	1.9	6.5
4D	24.	10.8	38.
5S	17.	7.9	27.

Table V. Neutral-ionic curve crossing radii for various Na electronic states in the Na + HCl reaction.

Na(nL)	IP{Na(nL)} (eV)	r_c (Å)	πr_c^2 (Å^2)
3S	5.138	2.41	18
3P	3.033	3.72	47
4D	0.854	8.60	232
5S	1.021	7.82	192

REFERENCES

1. E. H. Taylor and S. Datz, *J. Chem. Phys.* **23**, 1711 (1955).
2. C. H. Becker, P. Casavecchia, P. W. Tiedemann, J. J. Valentini, and Y. T. Lee, *J. Chem. Phys.* **73**, 2833 (1980).
3. K. Lacmann and D. R. Herschbach, *Chem. Phys. Lett.* **6**, 106 (1970).
4. J. G. Pruett, F. R. Grabiner, and P. R. Brooks, *J. Chem. Phys.* **63**, 1173 (1975).
5. M. W. Geis, H. Dispert, T. L. Budzynski, and P. R. Brooks, *State to State Chemistry*, P. R. Brooks and E. F. Hayes, eds., ACS Symposium Series No. 56, 103, American Chemical Society, Washington, DC (1977).
6. F. Heismann and H. J. Loesch, *Chem. Phys.* **64**, 43 (1982).
7. T. J. Odiorne, P. R. Brooks, and J. V. V. Kasper, *J. Chem. Phys.* **55**, 1980 (1971).
8. M. Hoffmeister, L. Potthast, and H. J. Loesch, *Chem. Phys.* **78**, 369 (1983).
9. H. H. Dispert, M. W. Geis, and P. R. Brooks, *J. Chem. Phys.* **70**, 5317 (1979).
10. B. A. Blackwell, J. C. Polanyi, and J. J. Sloan, *Chem. Phys.* **30**, 299 (1978).
11. M. F. Vernon, H. Schmidt, P. S. Weiss, M. H. Covinsky, and Y. T. Lee, *J. Chem. Phys.* **84**, 5580 (1986).
12. M. F. Vernon, Ph.D. Thesis, Univ. of California, Berkeley (1983).
13. P. S. Weiss, Ph.D. Thesis, Univ. of California, Berkeley (1986).
14. R. Düren, U. Lackschewitz, S. Milosevic, H. Pankin, and N. Schirawski, *Chem. Phys. Lett.* **143**, 45 (1988).
15. M. M. L. Chen and H. F. Schaefer III, *J. Chem. Phys.* **72**, 4376 (1980).
16. Y. Zeiri and M. Shapiro, *Chem. Phys.* **31**, 217 (1978).
17. M. Shapiro and Y. Zeiri, *J. Chem. Phys.* **70**, 5264 (1979).
18. Y. Zeiri, M. Shapiro, and E. Pollack, *Chem. Phys.* **60**, 239 (1981).
19. I. NoorBatcha and N. Sathyamurthy, *J. Chem. Phys.* **76**, 6447 (1982).
20. I. NoorBatcha and N. Sathyamurthy, *J. Am. Chem. Soc.* **104**, 1766 (1982).
21. I. NoorBatcha and N. Sathyamurthy, *Chem. Phys. Lett.* **93**, 432 (1982).
22. S. Carter and J. N. Murrell, *Mol. Phys.* **41**, 567 (1980).
23. A. Sevin, P. C. Hiberty, and J.-M. Lefour, *J. Am. Chem. Soc.* **109**, 1845 (1987).

24. M. M. Gallo and D. R. Yarkony, *J. Chem. Phys.* **86**, 4990 (1987).

25. D. R. Yarkony, *Int. J. Quantum Chem.* **31**, 91 (1987).

26. G. G. Balint-Kurti and R. N. Yardley, *Faraday Disc. Chem. Soc.* **62**, 77 (1977).

27. R. R. Herm, in *Alkali Halide Vapors: Structure, Spectra, and Reaction Dynamics*, 189, Academic Press, New York (1979), and references therein.

28. W. A. Lester, Jr. and M. Krauss, *J. Chem. Phys.* **52**, 4775 (1970).

29. Y. T. Lee, J. D. McDonald, P. R. LeBreton, and D. R. Herschbach, *Rev. Sci. Inst.* **40**, 1402 (1969).

30. P. E. Siska, J. M. Parson, T. P. Schaefer, and Y. T. Lee, *J. Chem. Phys.* **55**, 5762 (1971).

31. S. Gerstenkorn and P. Luc, *Atlas du Spectre d'Absorption de la Molecule d'Iode*, Editions du CNRS, Paris (1978).

32. For an explanation of the cross-correlation technique, see: G. Comsa, R. David, and B. J. Schumacher, *Rev. Sci. Intrum.* **52**, 789 (1981).

33. T. T. Warnock and R. B. Bernstein, *J. Chem. Phys.* **49**, 1878 (1968).

34. R. J. Buss, Ph.D. Thesis, Univ. of California, Berkeley (1979).

35. W. L. Wiese, M. W. Smith, and B. M. Miles, *Atomic Transition Probabilities Volume II: Sodium Through Calcium*, Natl. Stand. Ref. Data Ser., Nat. Bur. Stand. (U.S.), Washington, DC (1969).

36. O. S. Heavens, *J. Opt. Soc.* **51**, 1058 (1961).

37. A. Fischer and I. V. Hertel, *Z. Phys. A* **304**, 103 (1982).

38. I. V. Hertel and W. Stoll, *Adv. At. Mol. Phys.* **13**, 113 (1978), and references therein.

39. G. Jamieson, W. Reiland, C. P. Schulz, H.-U. Tittes, and I. V. Hertel, *J. Chem. Phys.* **81**, 5805 (1984).

40. Calculated from the diatomic molecular dissociation constants in K. P. Huber and G. Herzberg, *Molecular Spectra and Molecular Structure, IV. Constants of Diatomic Molecules*, Van Nostrand Reinhold, Co., New York (1979).

41. D. C. Frost and C. A. McDowell, *J. Chem. Phys.* **29**, 503 (1958).

42. J. H. Birely, R. R. Herm, K. R. Wilson, and D. R. Herschbach, *J. Chem. Phys.* **47**, 993 (1967).

43. C. H. Chen, H. Haberland, and Y. T. Lee, *J. Chem. Phys.* **61**, 3095 (1974).

44. J. N. Bardsley and J. M. Wadehra, *J. Chem. Phys.* **78**, 7227 (1983).

45. J. L. Magee, *J. Chem. Phys.* **8**, 687 (1940).

46. R. D. Levine and R. B. Bernstein, *Molecular Reaction Dynamics*, 86, Oxford University Press, New York (1974).

FIGURE CAPTIONS

Figure 1. Schematic of the optical pumping system used for the Na excitation. The symbols for optional components are in parentheses. The components are: (BS) Beam Splitter, (M) Mirror, (GT) Glan-Thompson Prism, ($\lambda/4$) Quarter-Wave Plate, (FP) Fabry-Perot Etalon, (S) Shutter, (F) Filter, (PMT) Photomultiplier and/or Fluorescence Monitor, (Na) Sodium Source, (2) Secondary Molecular Beam, and (MS) Quadrupole Mass Spectrometer.

Figure 2. The sodium atomic levels relevant to the optical pumping. The fine and hyperfine structure levels are not shown. The relative populations of the various sodium levels as calculated in ref. [39] for optically pumping the $Na(4^2D_{5/2})$ [$Na(4^2D_{5/2})$] state are as shown.

Figure 3. Newton velocity vector diagrams for $Na(3S,3P,4D,5S) + HCl \rightarrow NaCl + H$ at collision energies of a) 3.4 kcal/mole, b) 5.6 kcal/mole, and c) 16.3 kcal/mole. The sodium beam was seeded in a) argon, b) neon, and c) helium. The HCl beam was neat.

Figure 4. NaCl angular distributions for $Na(3S,3P,4D,5S) + HCl \rightarrow NaCl + H$ at a collision energy of 3.4 kcal/mole.

Figure 5. NaCl angular distributions for $Na(3S,3P,4D,5S) + HCl \rightarrow NaCl + H$ at a collision energy of 5.6 kcal/mole.

Figure 6. NaCl angular distributions for $Na(3S,3P,4D,5S) + HCl \rightarrow NaCl + H$ at a collision energy of 16.3 kcal/mole.

Figure 7. TOF distributions for NaCl angular distributions for $Na(4D) + HCl \rightarrow NaCl + H$ at a collision energy of 5.6 kcal/mole at the angles shown. The solid lines are the fit to the data generated from center-of-mass angular and translational energy distributions.

Figure 8. TOF distributions for NaCl angular distributions for $Na(5S) + HCl \rightarrow NaCl + H$ at a collision energy of 5.6 kcal/mole at the angles shown. The solid lines are the fit to the data generated from center-of-mass angular and translational energy distributions.

Figure 9. Laser polarization dependences of the NaCl reactive signal due to the $Na(4D) + HCl$ reaction at a collision energy of 5.6 kcal/mole for the angles shown in each frame. The solid lines are fits to the data.

Figure 10. NaBr angular distributions for $Na(3S,3P) + HBr \rightarrow NaBr + H$ at a collision energy of 3.0 kcal/mole.

Figure 11. NaBr angular distributions for Na(3S,3P) + HBr → NaBr + H at a collision energy of 5.3 kcal/mole.

Figure 12. NaBr angular distributions for Na(3S,3P) + HBr → NaBr + H at a collision energy of 20. kcal/mole.

Figure 13. NaCl angular distributions for Na(4D,5S) + HCl → NaCl + H at a collision energy of 5.6 kcal/mole. The solid lines are the fit to the data generated from center-of-mass angular and translational energy distributions.

Figure 14. Fit center-of-mass product translational energy distributions for: Na(3P) + HCl → NaCl + H at a collision energy of 5.4 kcal/mole from ref. [11], and Na(4D,5S) + HCl → NaCl + H at a collision energy of 5.6 kcal/mole.

Figure 15. Fit product NaCl center-of-mass scattering angular distributions at a collision energy of 5.6 kcal/mole for Na(4D,5S) + HCl.

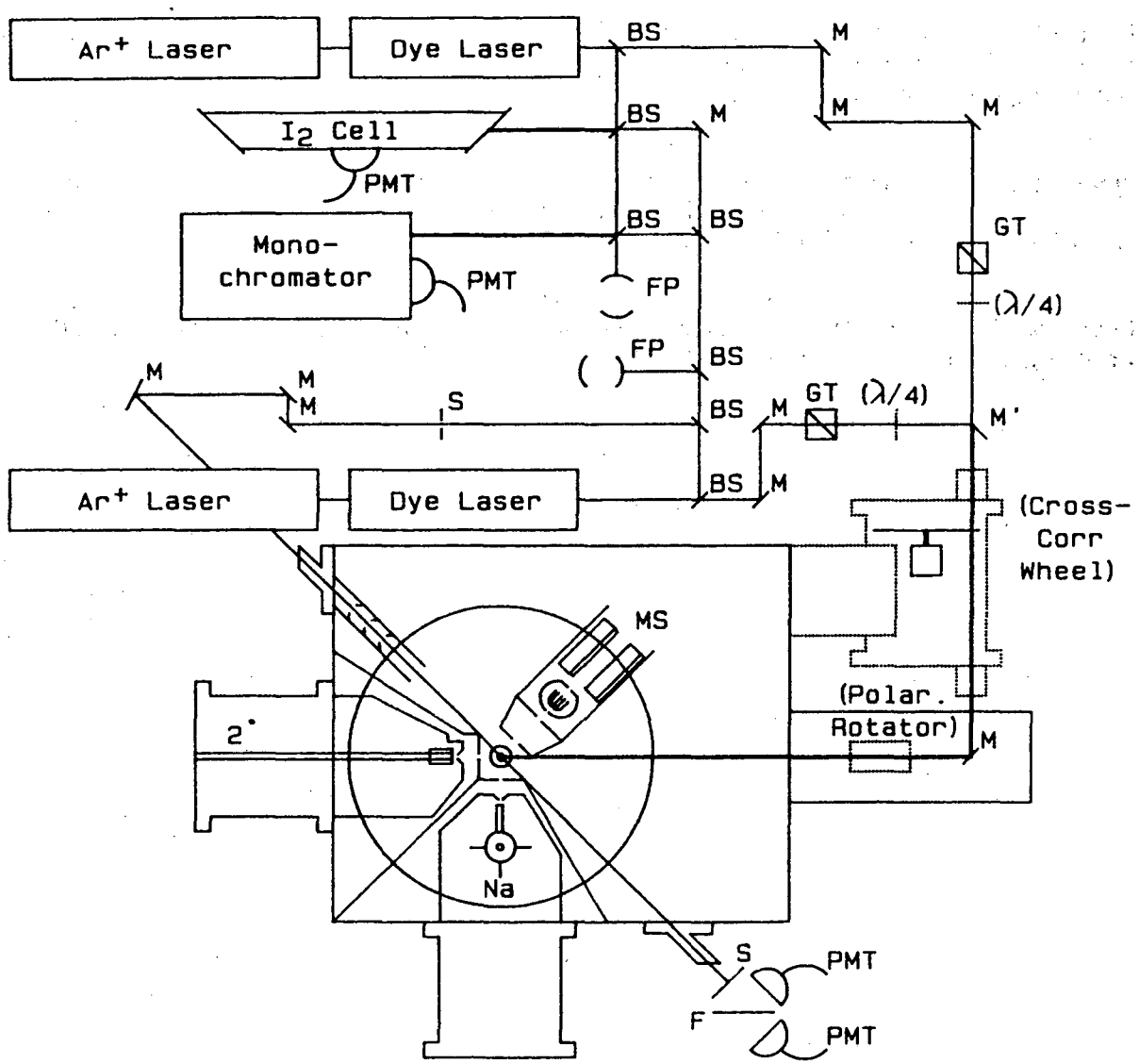

XBL 862-631

Fig. 1

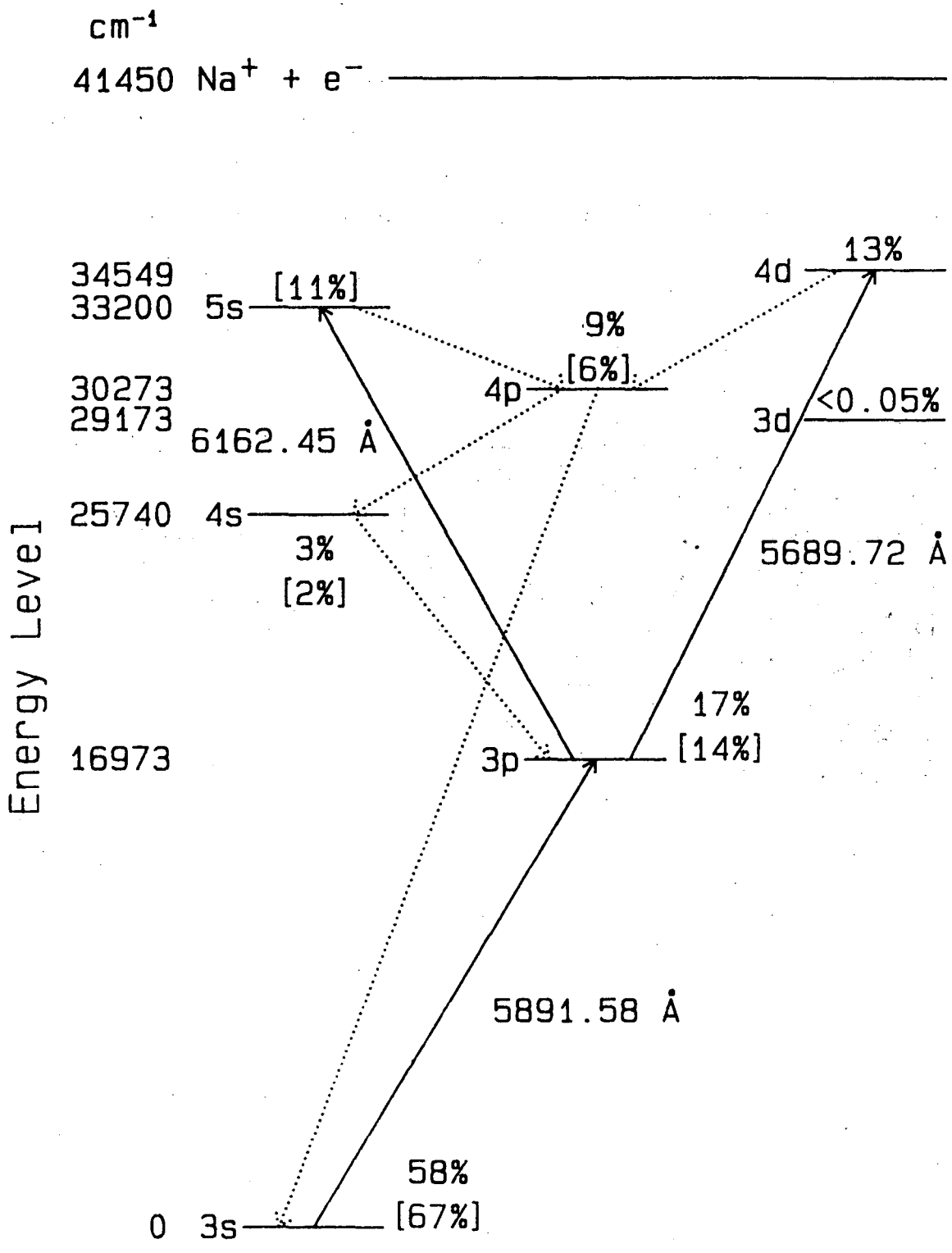

XBL 861-80

Fig. 2

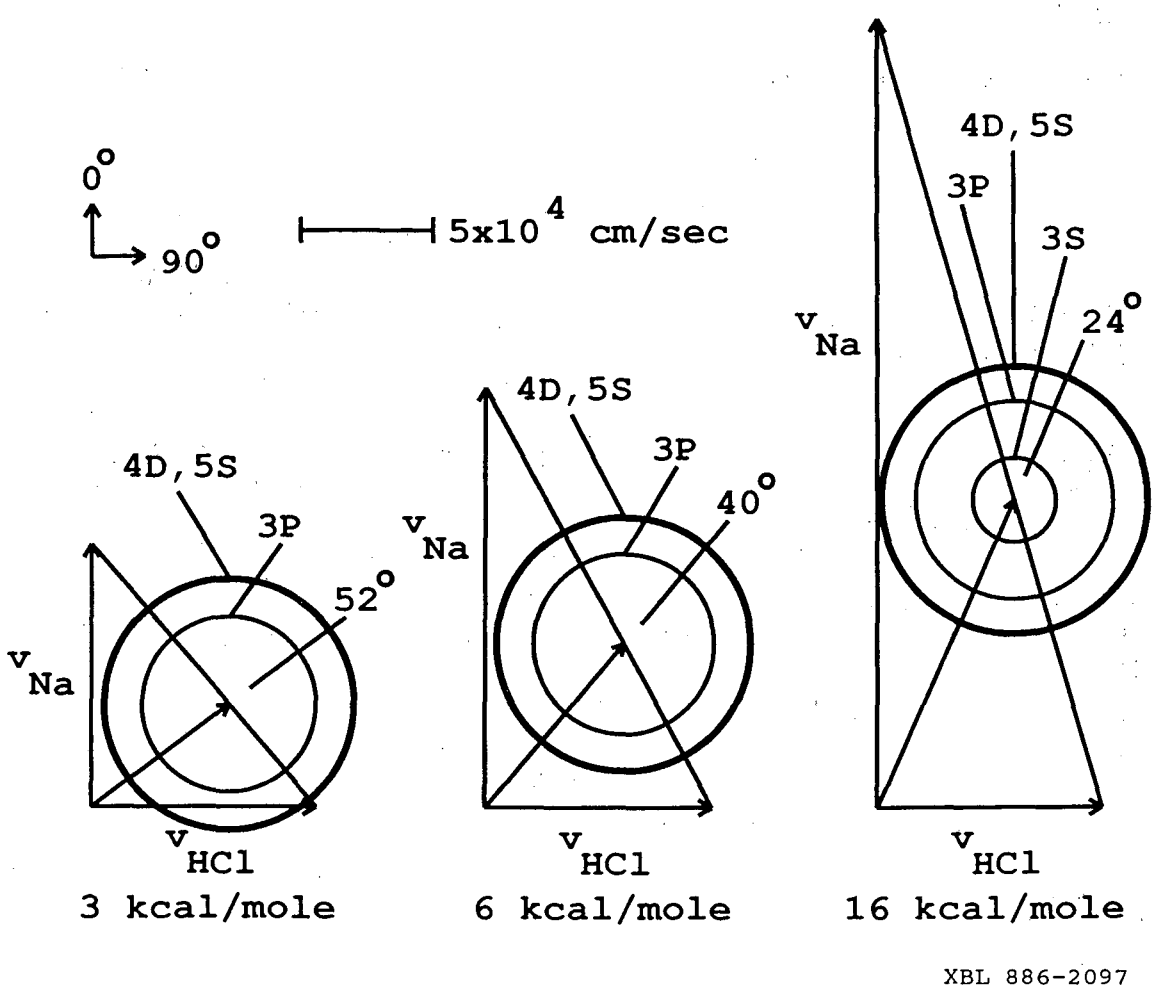

XBL 886-2097

Fig. 3

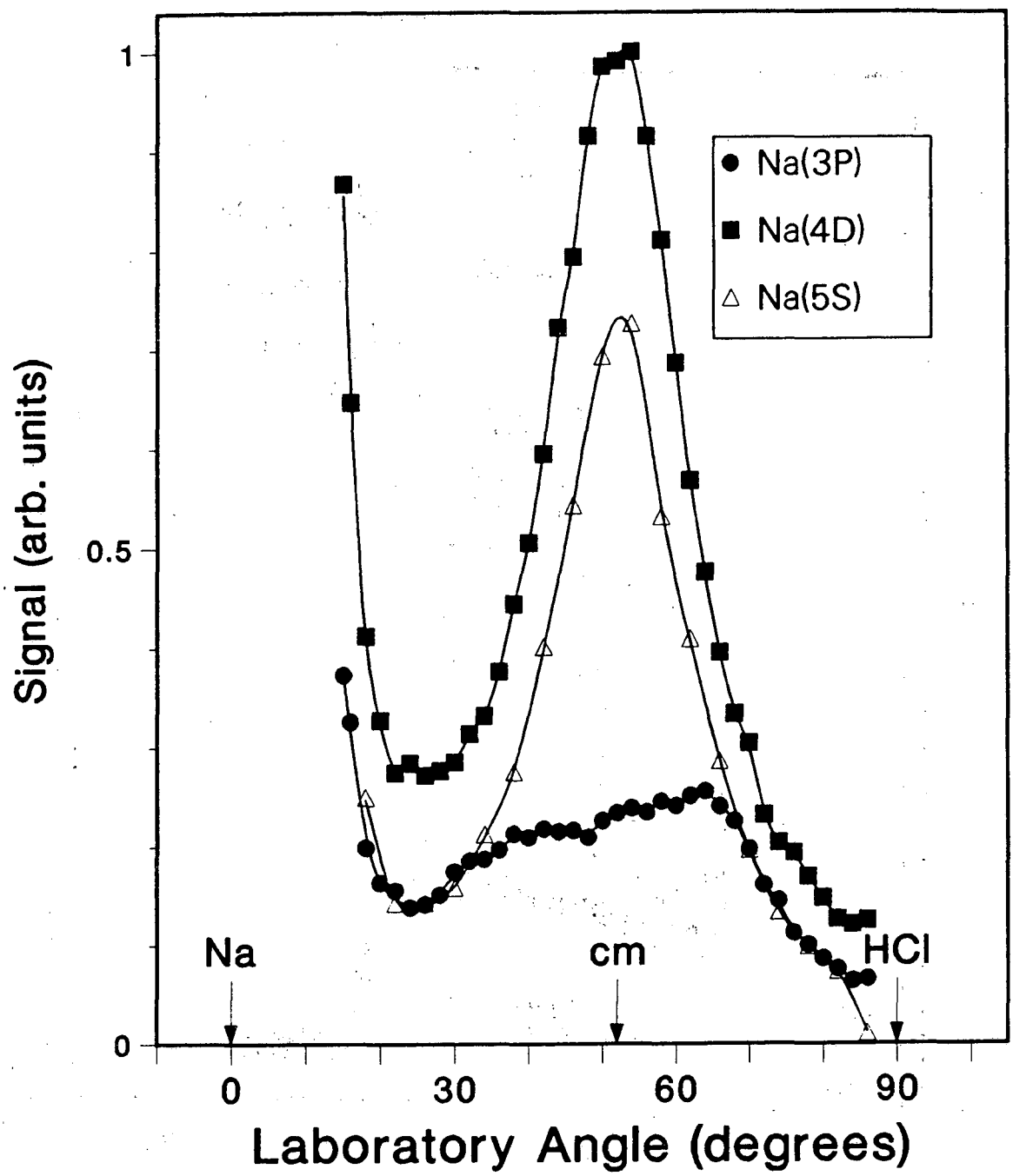

XBL 863-882

Fig. 4

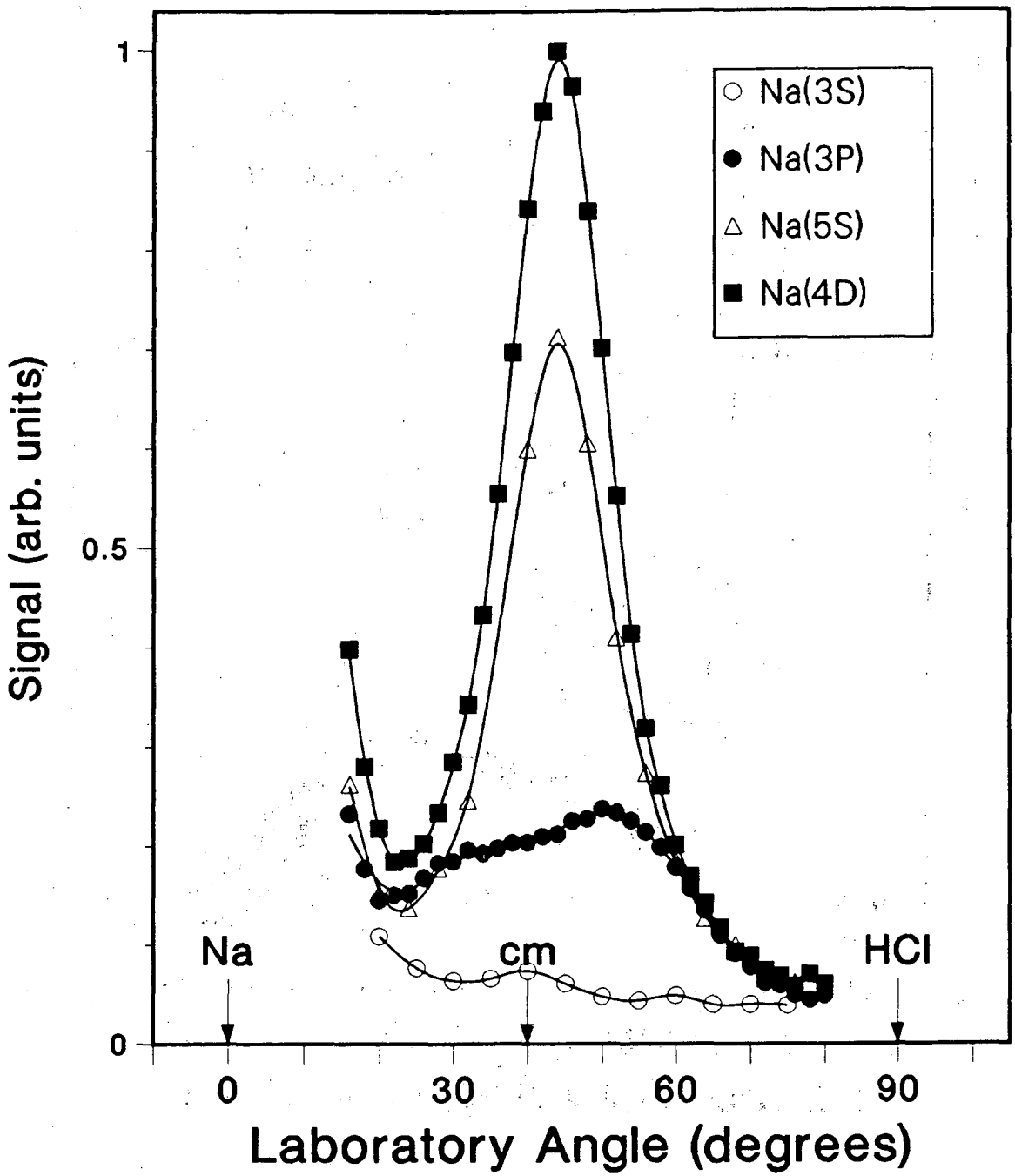

XBL 863-883

Fig. 5

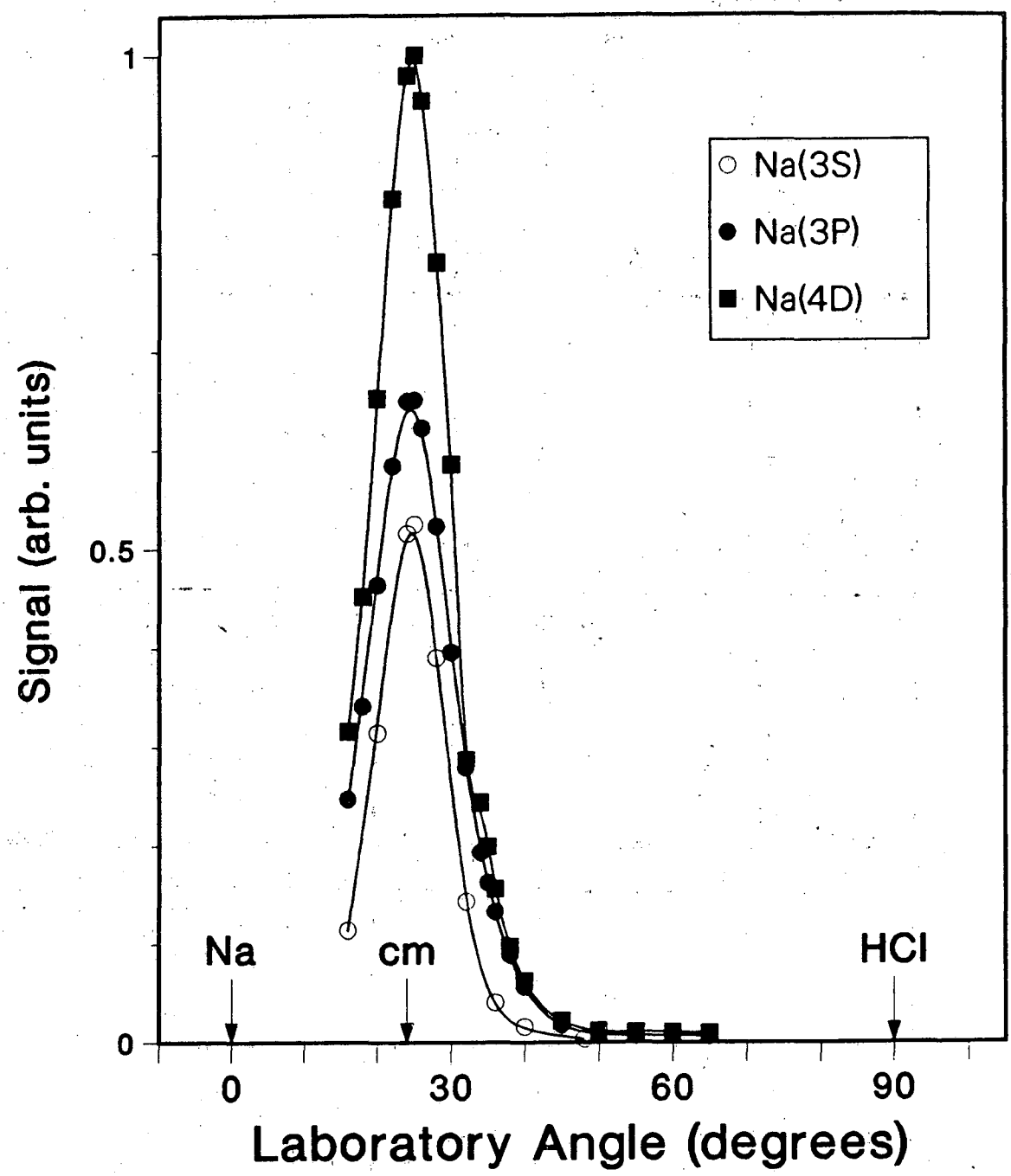

XBL 863-884

Fig. 6

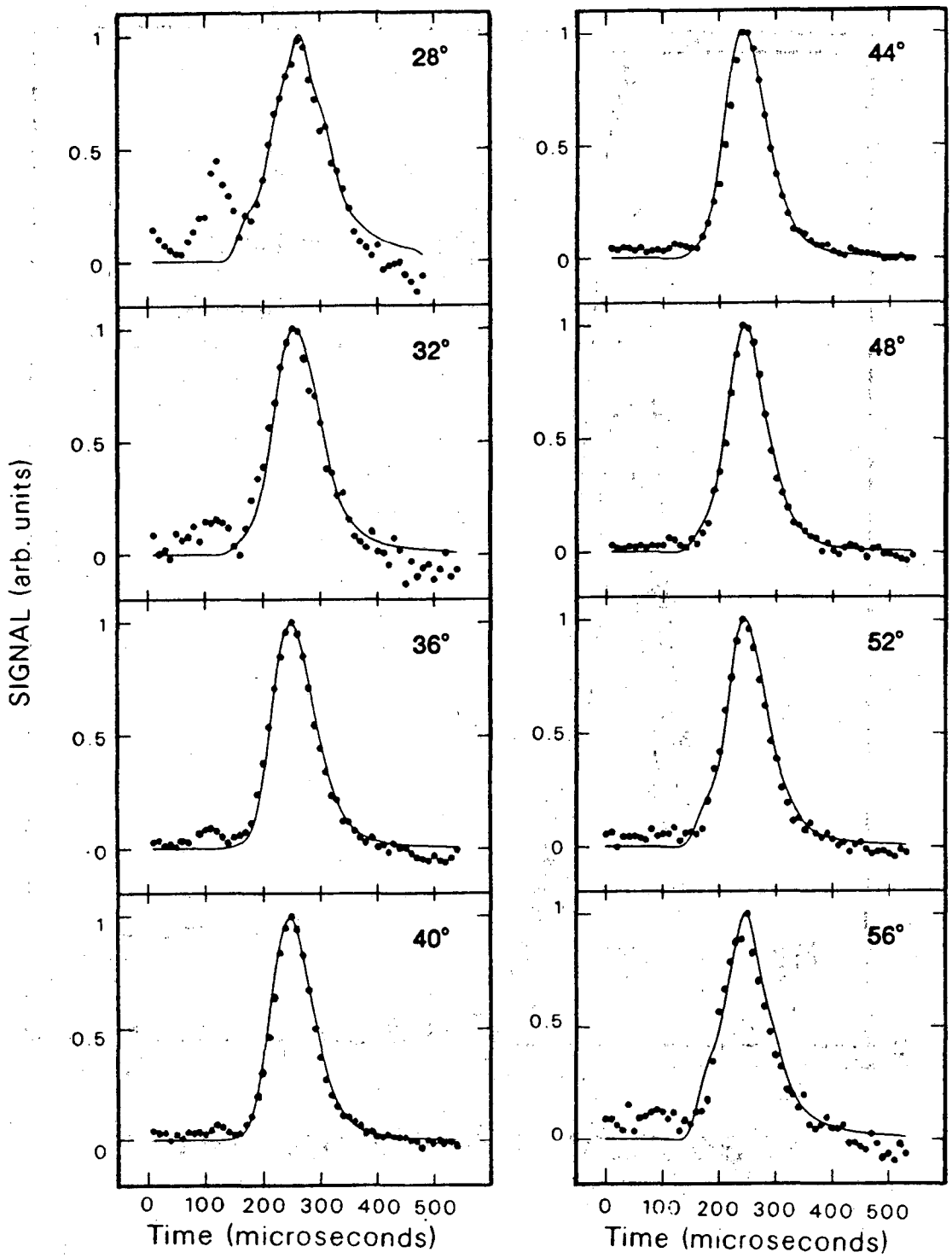

XBL 863-756A

Fig. 7

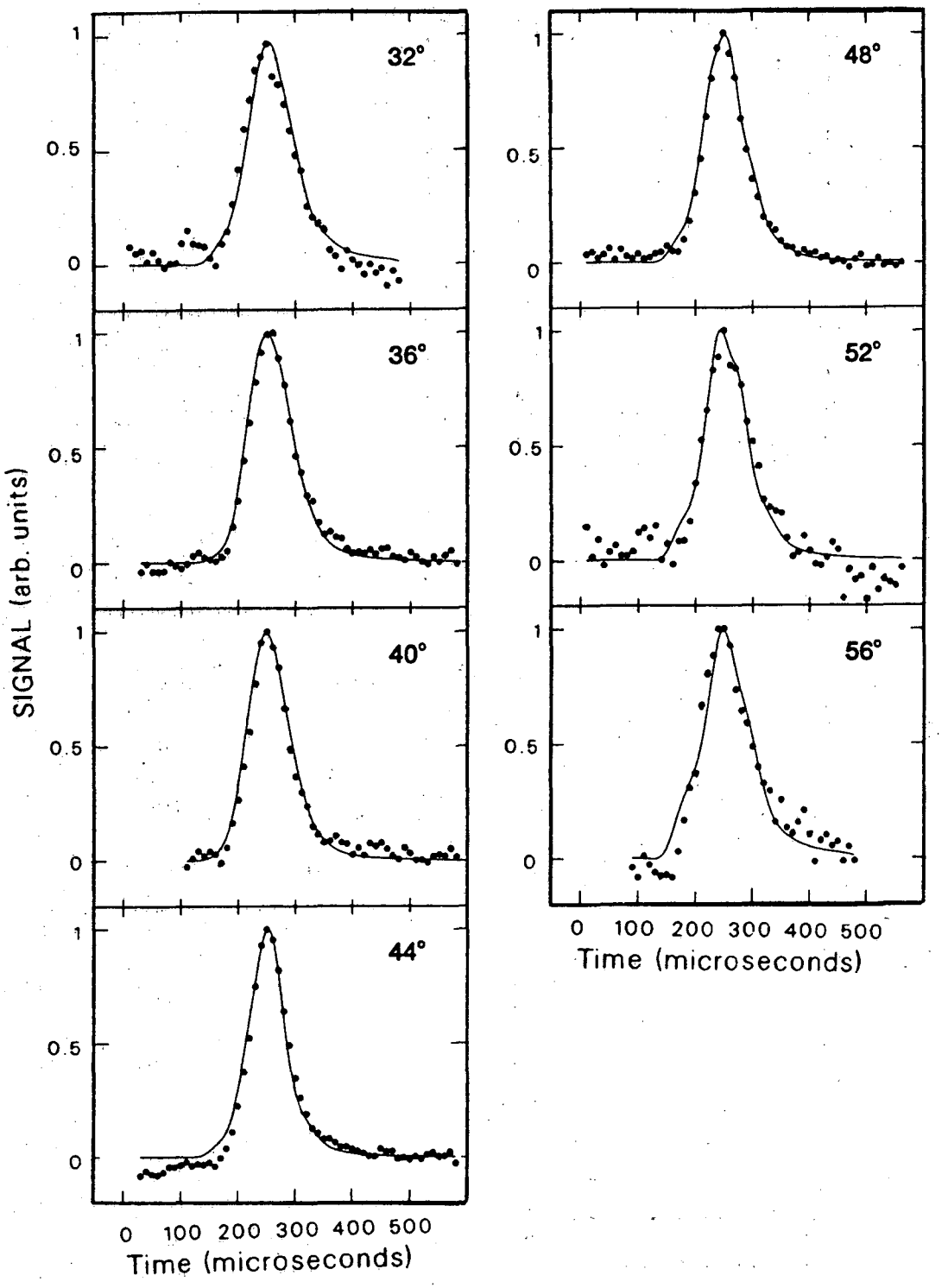

XBL 863-754A

Fig. 8

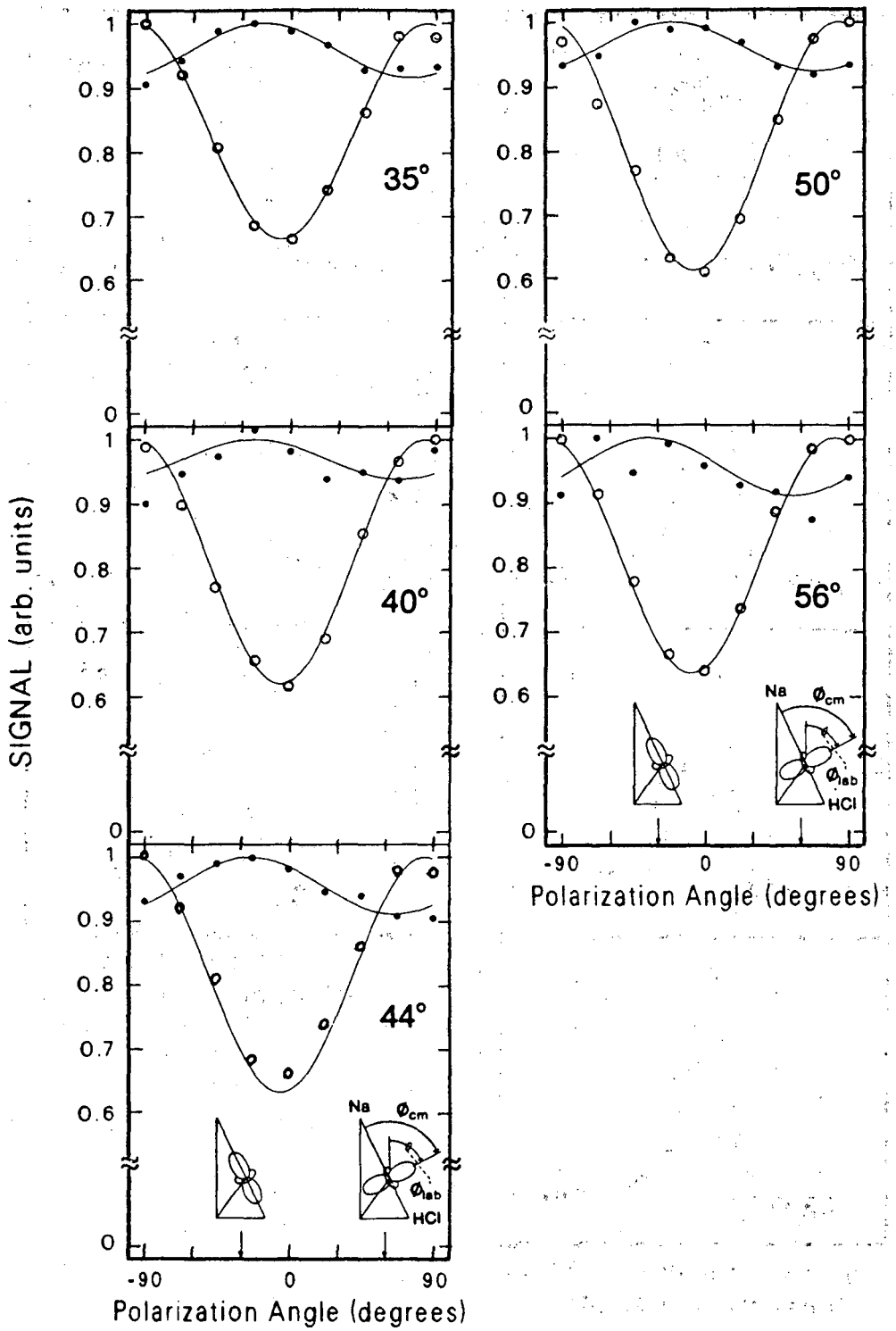

XBL 863-895 A

Fig. 9

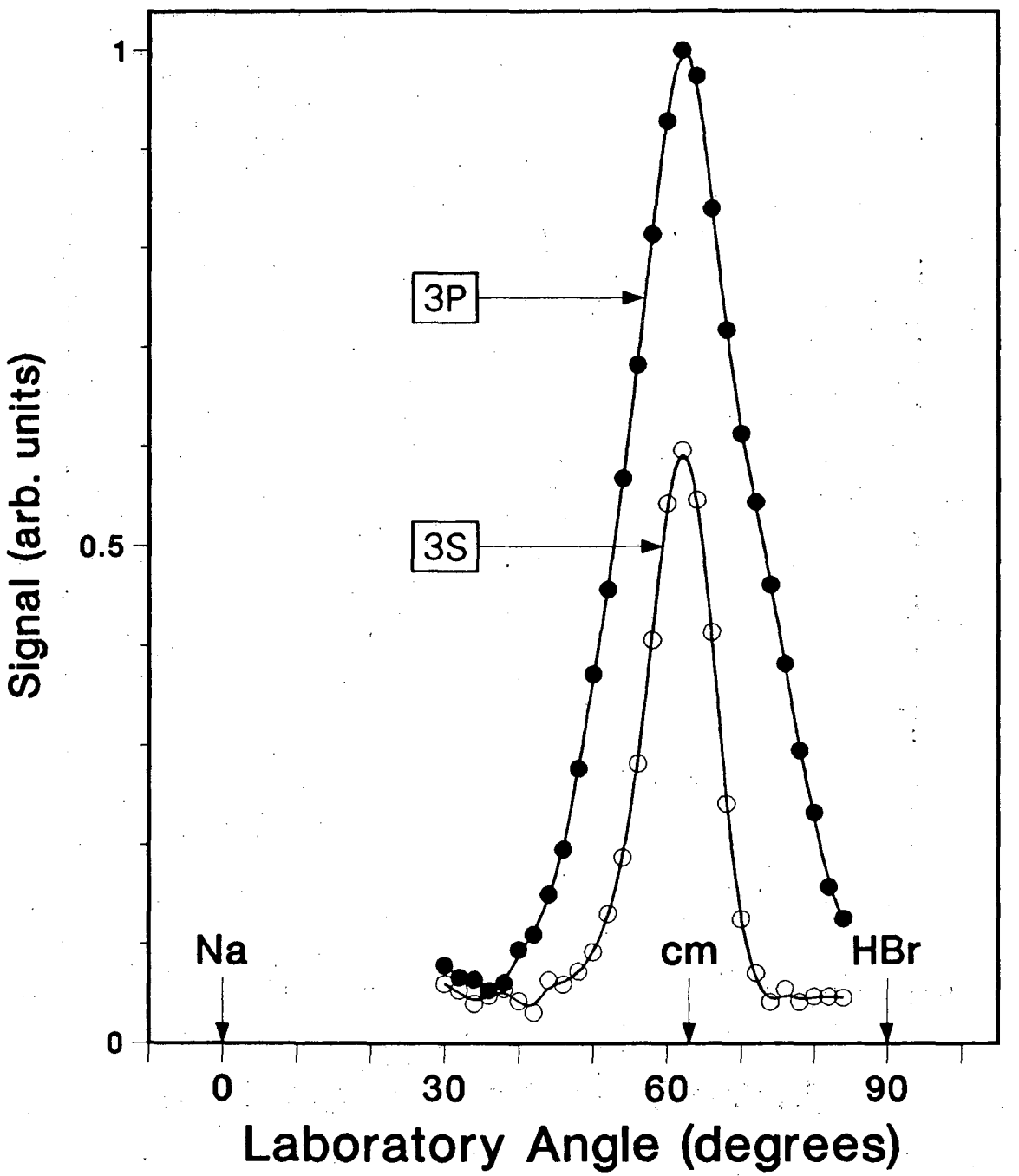

XBL 863-879

Fig. 10

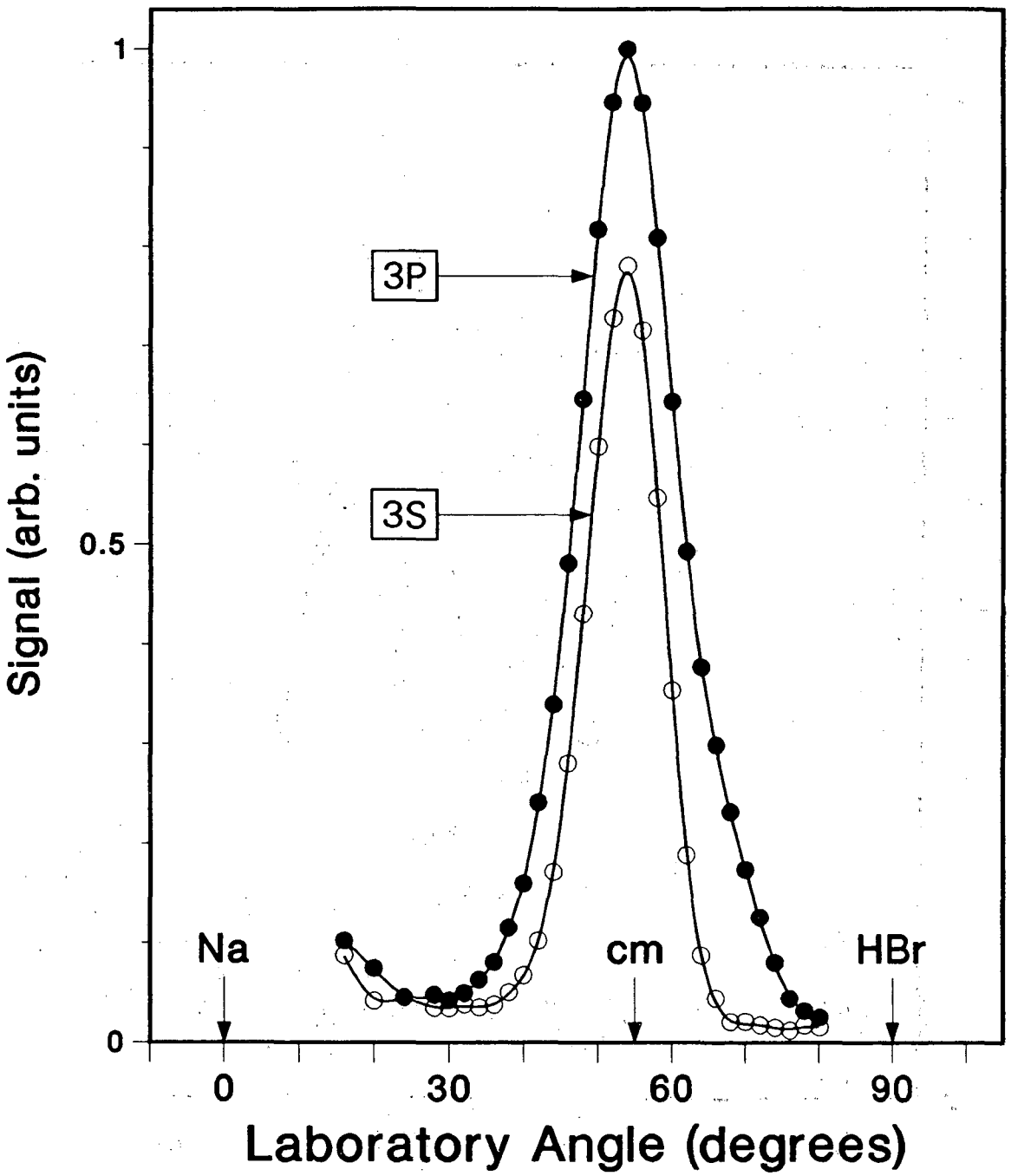

XBL 863-880

Fig. 11

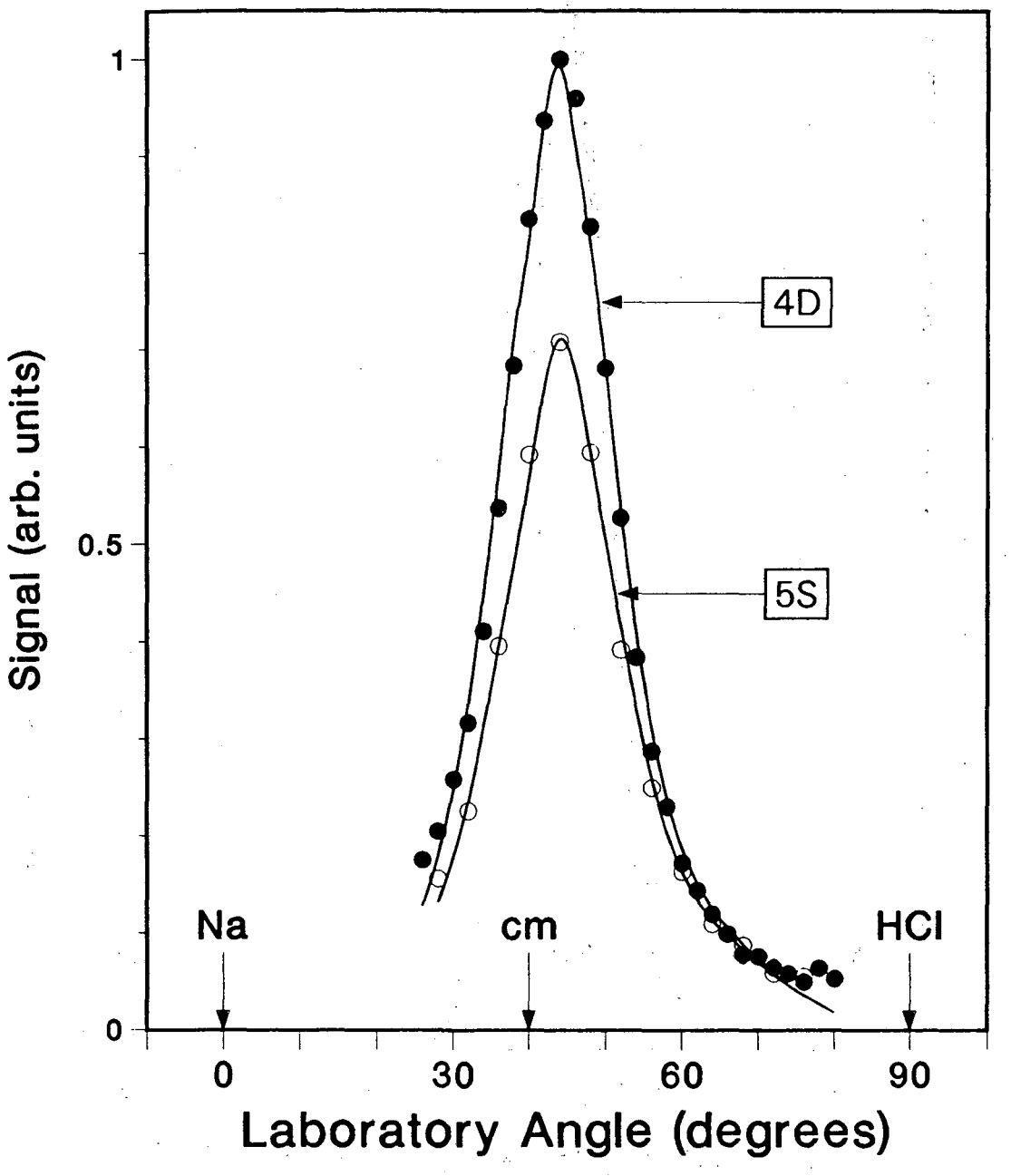

XBL 863-761

Fig. 12

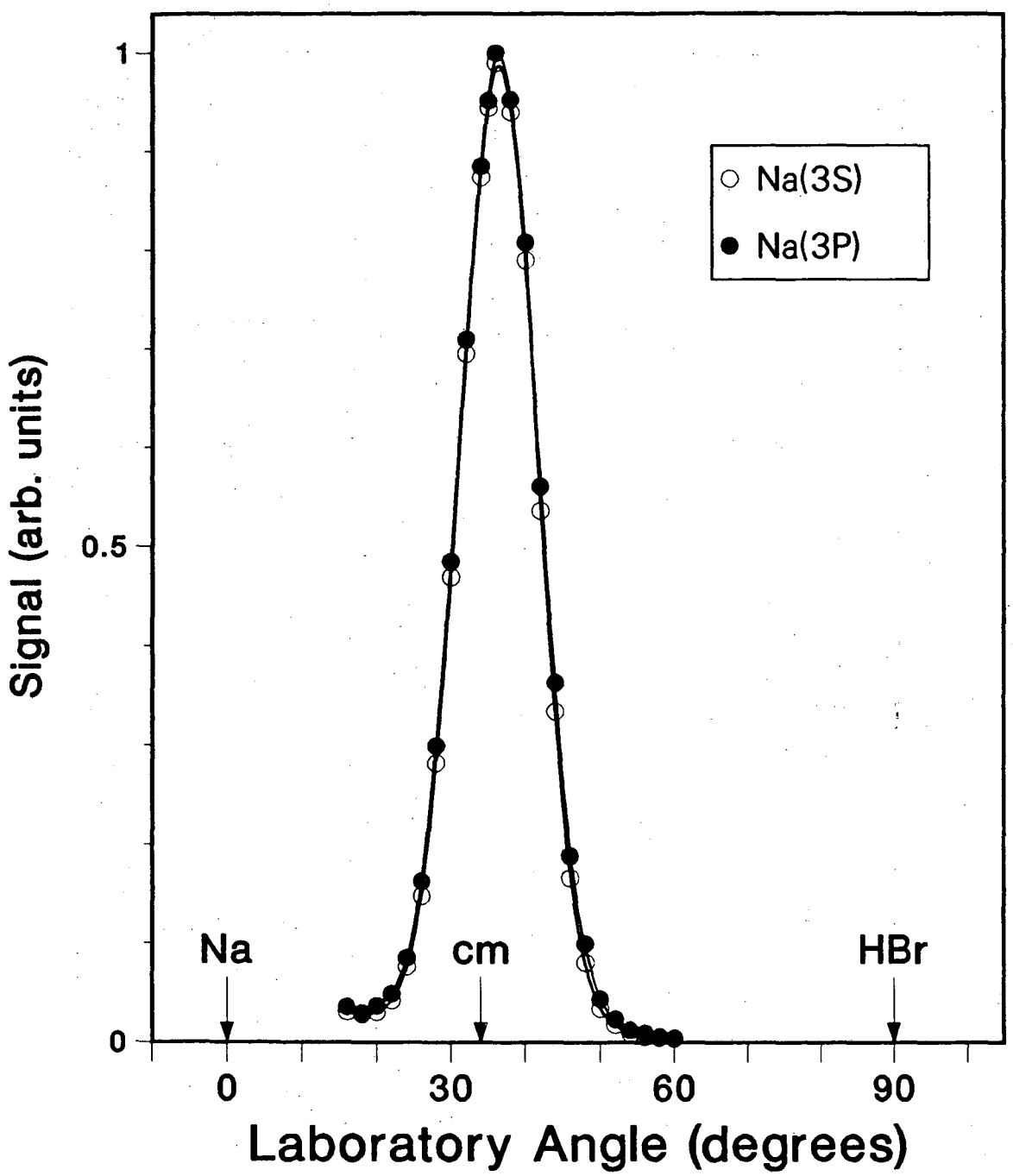

XBL 863-881

Fig. 13

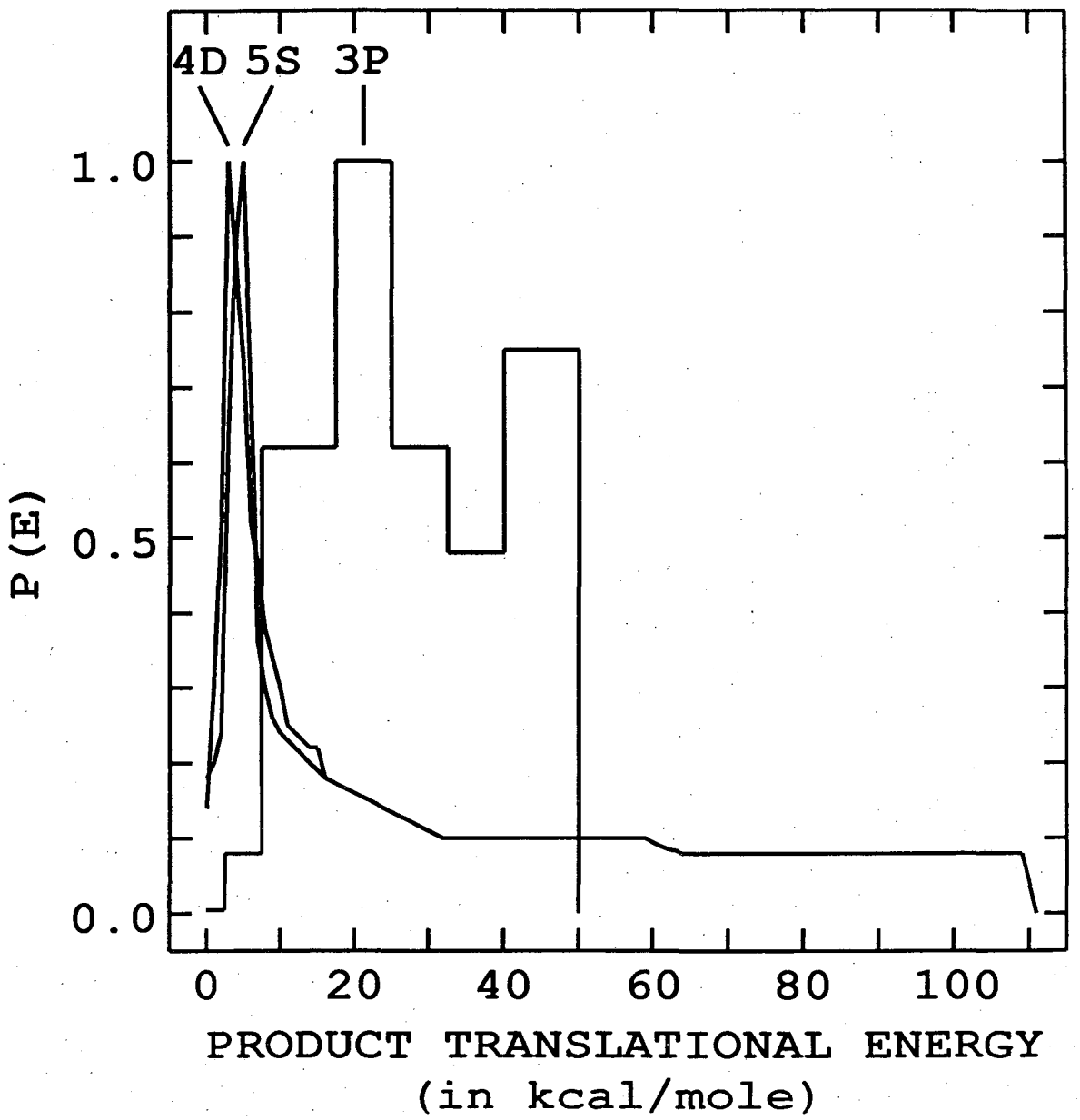

XBL 886-2098

Fig. 14

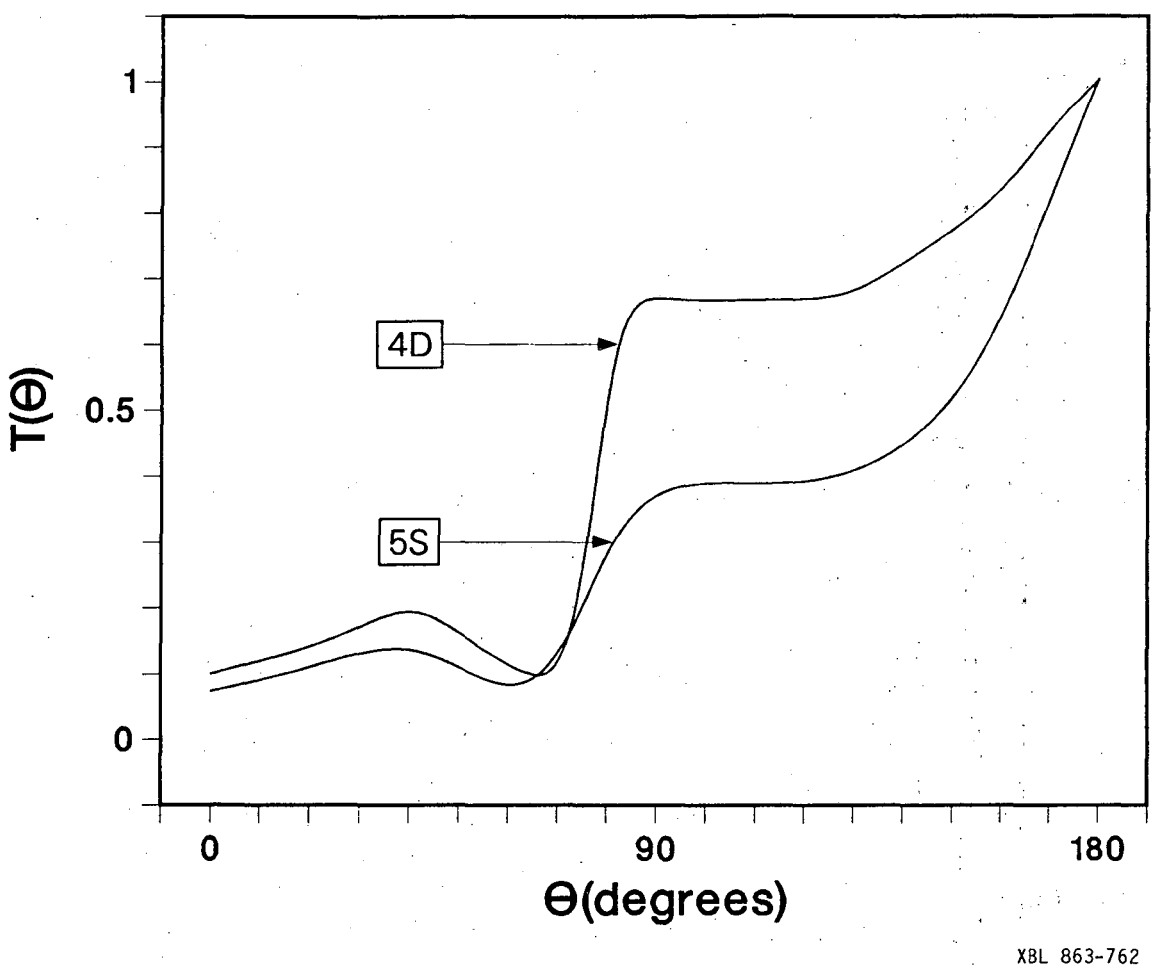

Fig. 15

LAWRENCE BERKELEY LABORATORY
TECHNICAL INFORMATION DEPARTMENT
UNIVERSITY OF CALIFORNIA
BERKELEY, CALIFORNIA 94720